Accepted Manuscript

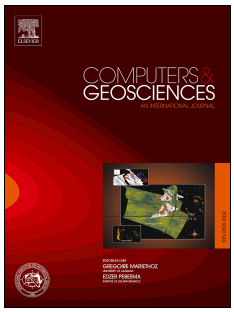

Uncertainty modelling and analysis of volume calculations based on a regular grid digital elevation model (DEM)

Chang Li, Qing Wang, Wenzhong Shi, Sisi Zhao

PII: S0098-3004(16)30732-4

DOI: 10.1016/j.cageo.2018.01.002

Reference: CAGEO 4075

To appear in: *Computers and Geosciences*

Received Date: 29 November 2016

Revised Date: 17 November 2017

Accepted Date: 10 January 2018

Please cite this article as: Li, C., Wang, Q., Shi, W., Zhao, S., Uncertainty modelling and analysis of volume calculations based on a regular grid digital elevation model (DEM), *Computers and Geosciences* (2018), doi: 10.1016/j.cageo.2018.01.002.

Uncertainty modelling and analysis of volume calculations based on a regular grid digital elevation model (DEM)

CHANG LI [1] *, Qing Wang [1] Wenzhong SHI [2] and Sisi ZHAO [1]
1 Key Laboratory for Geographical Process Analysis & Simulation, Hubei Province, and College of Urban and Environmental Science, Central China Normal University, Wuhan, China.
2 Joint Spatial Information Research Laboratory, The Hong Kong Polytechnic University and Wuhan University, Hong Kong and Wuhan, China.

The accuracy of earthwork calculations that compute terrain volume is critical to digital terrain analysis (DTA). The uncertainties in volume calculations (VCs) based on a DEM are primarily related to three factors: 1) model error (ME), which is caused by an adopted algorithm for a VC model, 2) discrete error (DE), which is usually caused by DEM resolution and terrain complexity, and 3) propagation error (PE), which is caused by the variables' error. Based on these factors, the uncertainty modelling and analysis of VCs based on a regular grid DEM are investigated in this paper. Especially, how to quantify the uncertainty of VCs is proposed by a confidence interval based on truncation error (TE). In the experiments, the trapezoidal double rule (TDR) and Simpson's double rule (SDR) were used to calculate volume, where the TE is the major ME, and six simulated regular grid DEMs with different terrain complexity and resolution (i.e. DE) were generated by a Gauss synthetic surface to easily obtain the theoretical true value and eliminate the interference of data errors. For PE, Monte-Carlo simulation techniques and spatial autocorrelation were used to represent DEM uncertainty. This study can enrich uncertainty modelling and analysis-related theories of geographic information science.

Keywords: Volume calculation; DTA; Uncertainty modelling; Truncation error; propagation; Terrain complexity; DEM

1 Introduction

For many disciplines, uncertainty has been recognized as an important part of basic theory. Goodchild (1992) identified GIScience as a set of fundamental scientific issues that are stimulated by or surround the use of digital computers to handle, process, analyse, store or access geographic information. Data serve as the carrier of information of an objective entity; approximately 70% of phenomena in the real world are position-related and can be described by spatial data (Shi 2009). Thus, the need for spatial data has increased in a rapidly changing world due to the widespread development and application of GISs (the major research and application tool of GIScience) (Li et al. 2012). However, the quality of geospatial data cannot be guaranteed because information gathering and processing suffer from various man-machine limitations (Goodchild and Jeansoulin 1998). These limitations create uncertainty in spatial data and these uncertainties may produce unforeseeable spatial analysis errors. Therefore, studying the uncertainty of spatial data is very important.

In past two decades, the study of the uncertainty of spatial data has achieved fruitful results, especially the study of the uncertainty of a digital elevation model (DEM) for digital terrain analysis (DTA) (LI, et al. 2005). As the focus of the study of spatial data uncertainty, the study of the uncertainty of a DEM is primarily concentrated in two aspects: a) the uncertainty modelling and analysis of DEM data sources (Carlisle 2005, James et al. 2007, Wheaton et al. 2010) and b) the uncertainty modelling and analysis of DEM interpolation (Shi et al. 2005, Shi and Tian 2006). Although some studies of the uncertainty of DEM applications have also

* Corresponding author, E-mail: lcshaka@126.com and lichang@mail.ccnu.edu.cn

been undertaken by several scholars (e.g., Zhou and Liu 2002, Zhou and Liu 2004, Zhou et al. 2006), these studies remain in a preliminary stage, and many research methods remain in an exploration stage (Wu et al. 2010). Aforementioned meaningful studies of the uncertainty of DEM applications not only have helped us accumulate experience, but also have provided us with great inspiration.

With the development of photogrammetry technologies in recent years (Sefercik et al. 2012, Wigmore 2014), the generation of a high-resolution DEM has become more convenient. Therefore, a considerable number of volume calculation (VC) models based on a DEM have been proposed (Arbogast et al. 2002, Lane et al. 2003, Tsutsui et al. 2007,). These models have significance for improving the accuracy and speed of earthwork VCs. However, the quantitative modelling and analysis of the uncertainty of VCs based on a DEM needs to be given more attention (Kerle, 2002). Therefore, additional theory and methods of uncertainty modelling and analyses in VC models based on a DEM need to be developed. Furthermore, the investigation of the uncertainties of VCs based on a DEM has important theoretical and practical significance.

In this paper, the uncertainty modelling and analysis of VCs based on a regular grid DEM was investigated. With considering DEM data source uncertainties, the main sources of uncertainties of VCs based on a DEM are primarily related to three aspects: a) model error (ME), which is defined as the difference between the true model and the approximate chosen, and here is usually caused by the adopted algorithm for VC models; b) discrete errors (DEs), which are usually caused by DEM resolution and terrain complexity; and c) propagation error (PE), which is cause by the variables' error. In this paper, trapezoidal double rule (TDR) and Simpson's double rule (SDR) are selected as the algorithms for calculating earthwork volumes from a regular grid DEM in that they are the most classical volume integral methods in numerical analysis. Moreover, the basic idea of experiment for the PE is to add random error to the simulated DEM. The contributions of this paper can be summarized as the following three aspects:

(a) Uncertainty models of VC based on a regular grid DEM are established by uncertainty quantification. Especially, confidence intervals of VCs based on truncation error (TE), TDR and SDR are proposed to quantify the uncertainty so that can develop the theory of DTA in GIScience;
(b) The formula of PE combined with a series of error propagation law is deduced and modelled for VC based on TDR and SDR. And, to simulate DEM error, Monte-Carlo method and spatial autocorrelation are used;
(c) This paper forms a guiding conclusion for VCs based on a DEM.

2 VCs and uncertainty modelling

In this section, we introduce the model of TDR and SDR, and the estimation of the range of the TE (i.e., uncertainty) for TDR and SDR.

2.1 *The theoretical model for VCs based on TDR and SDR*

According to double integral theory, volume (refer to figure 1) can be calculated by:

$$\iint_R f(x, y)\mathrm{d}x\mathrm{d}y \tag{1}$$

where $R = \{(x, y)|\ a \le x \le b, c \le y \le d\}$, for the constants a, b, c, and d, is a rectangular region in the plane (refer to figure 1).

As the terrain surface function is usually unknown or too complex, a numerical integration method is often used to approximately calculate the double integral in equation (1).

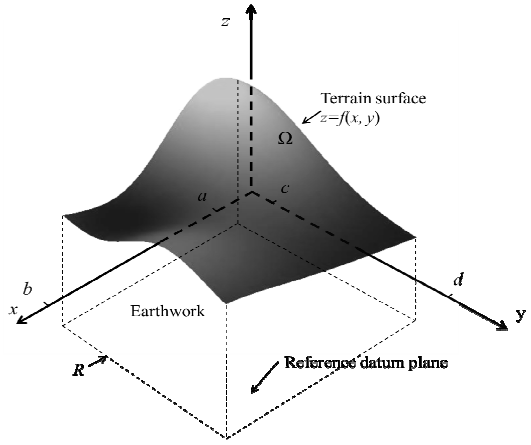

Figure 1: Schematic of VC

2.2 ***Practical model for VCs based on TDR and SDR***

2.2.1 *The approximate calculation method: TDR*

$$\int_a^b\int_c^d z(x,y)\mathrm{d}y\mathrm{d}x = M_{\mathrm{TDR}} + E_{\mathrm{TDR}} = \frac{hk}{4}\sum_{i=1}^{n-1}\sum_{j=1}^{m-1}[z(i,j)+z(i,j+1)+z(i+1,j)+z(i+1,j+1)] + E_{\mathrm{TDR}} \quad (2)$$

where n and m are number of partition of interval $[a, b]$ and $[c, d]$ respectively. E_{TDR} is the TE (i.e., uncertainty) of TDR; it can be expressed as follows (a detailed derivation is shown in Appendix 1)

$$E_{\mathrm{TDR}} = -\frac{(b-a)(d-c)}{12}[h^2\frac{\partial^2 f}{\partial x^2}(\xi,\eta) + k^2\frac{\partial^2 f}{\partial y^2}(\overline{\xi},\overline{\eta})] \quad (3)$$

where (ξ,η) and $(\overline{\xi},\overline{\eta})$ are any point in R.

2.2.2 *Approximate calculation method: SDR*

$$\begin{aligned}\int_a^b\int_c^d z(x,y)\mathrm{d}y\mathrm{d}x = M_{\mathrm{SDR}} + E_{\mathrm{SDR}} \approx \frac{hk}{9}\{&[z(1,1)+2\sum_{i=1}^{n-1}z(2i+1,1)\\ &+4\sum_{i=1}^{n}z(2i,1)+z(I,1)]\\ &+2[\sum_{j=1}^{m-1}z(1,2j+1)+2\sum_{j=1}^{m-1}\sum_{i=1}^{n}z(2i+1,2j+1)\\ &+4\sum_{j=1}^{m-1}\sum_{i=1}^{n}z(2i,2j+1)+\sum_{j=1}^{m-1}z(I,2j+1)]\\ &+4[\sum_{j=1}^{m}z(1,2j)+2\sum_{j=1}^{m}\sum_{i=1}^{n-1}z(2i+1,2j)\\ &+4\sum_{j=1}^{m}\sum_{i=1}^{n}z(2i,2j)+\sum_{j=1}^{m}z(I,2j)]\\ &+[z(1,J)+2\sum_{i=1}^{n-1}z(2i+1,J)+4\sum_{i=1}^{n}z(2i,J)\\ &+z(I,J)]\} + E_{\mathrm{SDR}}\end{aligned} \quad (4)$$

where M_{TDR} and M_{SDR} are measurement values calculated by TDR and SDR respectively. E_{SDR} is the TE (i.e., uncertainty) of SDR (detailed derivation in Appendix 2).

$$E_{\mathrm{SDR}} = -\frac{(b-a)(d-c)}{180}[h^4 \frac{\partial^4 f}{\partial x^4}(\overline{\eta},\overline{\mu}) + k^4 \frac{\partial^4 f}{\partial y^4}(\hat{\eta},\hat{\mu})] \quad (5)$$

where $(\overline{\eta},\overline{\mu})$ and $(\hat{\eta},\hat{\mu})$ are any point in R.

According to equation (3) and equation (5), point set (x_i, y_j, $f(x_i, y_j)$) is the key to using these equations to calculate the double integral. For a regular grid DEM, the point set is expressed as (i, j, $z(i, j)$)(i = 1, 2, 3…, I; j = 1, 2, 3,…, J). Here, I is the rows of the grid point of a regular grid DEM, and J is the columns of the grid point of a regular grid DEM. Thus, the step size h and k (refer to Figure 2) can be defined as:

$$h = \frac{(b-a)}{I-1} \quad \text{and} \quad k = \frac{(d-c)}{J-1} \quad (6)$$

Here, the value of variable a and variable b is shown in Figure 2.

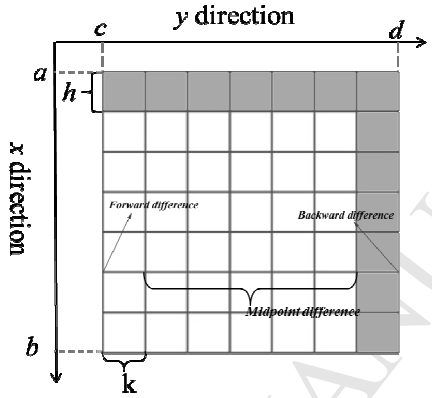

Figure 2. 2D representation of regular grid DEM (the coordinate is an image coordinate)

For TDR, the value of n and m can be directly replaced by I and J. For SDR, the value of n and m should be calculated by the following formulas:

$$n = \left[(b-a)/2h\right] \quad \text{and} \quad m = \left[(d-c)/2k\right] \quad (7)$$

x_i and y_j can be calculated by the following formulas:

$$x_i = a + (i-1)h \quad \text{and} \quad y_j = c + (j-1)k \quad (8)$$

Here, i = 1, 2, 3…, I; j = 1, 2, 3,…, J.

2.3 *Estimation of the confidence intervals for MEs of TDR and SDR*

Model error is defined as the difference between the true model and the approximate chosen (e.g. TDR or SDR). According to equation (3) and equation (5), the value of the TE is affected by four factors: the step sizes h and k and the partial derivative of the x direction and the y direction. The step sizes h and k is generally known but due to (ξ,η), $(\overline{\xi},\overline{\eta})$, $(\overline{\eta},\overline{\mu})$ and $(\hat{\eta},\hat{\mu})$, all cannot be clearly quantified and the partial derivative is often difficult to obtain. Thus, a difference method is employed to calculate the partial derivative. According to the mathematical principles of the simple numerical differentiation, we calculate the first-order partial derivative for each grid node. Based on the results of the first-order partial derivatives, a second-order partial derivative is calculated by re-applying the numerical differentiation method. The fourth-order partial derivative also can be calculated by the same method. When the maximum of a partial derivative is known, the TE range of TDR and SDR can be estimated by equation (3) and equation (5).

$$
\begin{aligned}
|E_{\mathrm{TDR}}| &= \left| -\frac{(b-a)(d-c)}{12}\left[h^2 \frac{\partial^2 f}{\partial x^2}(\xi,\eta) + k^2 \frac{\partial^2 f}{\partial y^2}(\bar{\xi},\bar{\eta}) \right] \right| \\
&\le \left| \frac{(b-a)(d-c)}{12} \right| \left[h^2 \left| \frac{\partial^2 f}{\partial x^2}(\xi,\eta) \right| + k^2 \left| \frac{\partial^2 f}{\partial y^2}(\bar{\xi},\bar{\eta}) \right| \right] \\
&\le \left| \frac{(b-a)(d-c)}{12} \right| \left(h^2 |\mathrm{Max}_1| + k^2 |\mathrm{Max}_2| \right) = \mathrm{AMTE}_{\mathrm{TDR}}
\end{aligned} \tag{9}
$$

$$
\begin{aligned}
|E_{\mathrm{SDR}}| &= \left| -\frac{(b-a)(d-c)}{180}\left[h^4 \frac{\partial^4 f}{\partial x^4}(\bar{\eta},\bar{\mu}) + k^4 \frac{\partial^4 f}{\partial y^4}(\hat{\eta},\hat{\mu}) \right] \right| \\
&\le \left| \frac{(b-a)(d-c)}{180} \right| \left[h^4 \left| \frac{\partial^4 f}{\partial x^4}(\bar{\eta},\bar{\mu}) \right| + k^4 \left| \frac{\partial^4 f}{\partial y^4}(\hat{\eta},\hat{\mu}) \right| \right] \\
&\le \left| \frac{(b-a)(d-c)}{180} \right| \left[h^4 |\mathrm{Max}_3| + k^4 |\mathrm{Max}_4| \right] = \mathrm{AMTE}_{\mathrm{SDR}}
\end{aligned} \tag{10}
$$

where |•| is an absolute value symbol; $|\mathrm{Max}_1|$, $|\mathrm{Max}_2|$, $|\mathrm{Max}_3|$ and $|\mathrm{Max}_4|$ are the maximum absolute values of $\left|\frac{\partial^2 f}{\partial x^2}(\xi,\eta)\right|$, $\left|\frac{\partial^2 f}{\partial y^2}(\bar{\xi},\bar{\eta})\right|$, $\left|\frac{\partial^4 f}{\partial x^4}(\bar{\eta},\bar{\mu})\right|$ and $\left|\frac{\partial^4 f}{\partial y^4}(\hat{\eta},\hat{\mu})\right|$, respectively; $\mathrm{AMTE}_{\mathrm{TDR}}$ and $\mathrm{AMTE}_{\mathrm{SDR}}$ mean absolute-maximum truncation error (AMTE) corresponding to TDR and SDR respectively.

Then, measurement uncertainty (uncertainty quantification) of VCs based on TDR and SDR can be calculated by "measured value" ± "uncertainty", so we have:

$$
\left(M_{\mathrm{TDR}} \pm \mathrm{AMTE}_{\mathrm{TDR}} \right) \quad \text{and} \quad \left(M_{\mathrm{SDR}} \pm \mathrm{AMTE}_{\mathrm{SDR}} \right) \tag{11}
$$

Hence, only considering the MEs of TDR and SDR, 100% confidence intervals of VCs based on the uncertainty of TE, the methods of TDR and SDR can be determined by Formula (11).

Absolute error (AE) is employed to estimate the accuracy of VC for DEM.

$$
\varepsilon_{\mathrm{TDR}} = \left| T - M_{\mathrm{TDR}} \right| \quad \text{and} \quad \varepsilon_{\mathrm{SDR}} = \left| T - M_{\mathrm{SDR}} \right| \tag{12}
$$

where T means true value; $\varepsilon_{\mathrm{TDR}}$ and $\varepsilon_{\mathrm{SDR}}$ are measurement values calculated by TDR and SDR respectively; and |•| is an absolute value symbol.

2.4 *VCs error propagation based on TDR and SDR*

In this paper, the error propagation law is used to evaluate the influence of the DEM grid point coordinate error (x, y) and elevation error (z) on the calculation accuracy.

2.4.1 *Error propagation based on TDR*

Suppose the $f(x_i, y_j)$, $f(x_i, y_j+1)$, $f(x_i+1, y_j)$, $f(x_i+1, y_j+1)$ correspond to the elevation values of four grid points in the formula (2) on a DEM grid unit respectively. First set:

$$
\begin{aligned}
\boldsymbol{K} &= \left[\frac{hk}{4} \quad \frac{hk}{4} \quad \frac{hk}{4} \quad \frac{hk}{4} \right] \\
\boldsymbol{X} &= \left[f(x_i, y_j) \quad f(x_i, y_{j+1}) \quad f(x_{i+1}, y_j) \quad f(x_{i+1}, y_{j+1}) \right]^{\mathrm{T}}
\end{aligned} \tag{13}
$$

Then the volume of a DEM grid cell can be expressed as:

$$
V_{\mathrm{TDR}} = \boldsymbol{K}\boldsymbol{X} \tag{14}
$$

where V_{TDR} is a volume of a DEM grid unit based on TDR; $\boldsymbol{K}$ is a covariance matrix of vector $\boldsymbol{X}$, and $\boldsymbol{X}$ is a variable vector.

According to the error propagation law of linear function:

$$
m_v^2 = \boldsymbol{K}\boldsymbol{D}_{XX}\boldsymbol{K}^{\mathrm{T}} \tag{15}
$$

where m_v^2 is a variance of V_{TDR}; $\boldsymbol{K}^{\mathrm{T}}$ is the transpose vector of $\boldsymbol{K}$; $\boldsymbol{D}_{XX}$ is a covariance matrix of variables and can be expressed as:

$$\boldsymbol{D}_{XX}=\begin{bmatrix}\sigma_{f_1}^2 & \sigma_{f_1f_2} & \sigma_{f_1f_3} & \sigma_{f_1f_4}\\ \sigma_{f_2f_1} & \sigma_{f_2}^2 & \sigma_{f_2f_3} & \sigma_{f_2f_4}\\ \sigma_{f_3f_1} & \sigma_{f_3f_2} & \sigma_{f_3}^2 & \sigma_{f_3f_4}\\ \sigma_{f_4f_1} & \sigma_{f_4f_2} & \sigma_{f_4f_3} & \sigma_{f_4}^2\end{bmatrix} \tag{16}$$

where f_1, f_2, f_3, f_4 are $f(x_i, y_j)$, $f(x_i, y_{j+1})$, $f(x_{i+1}, y_j)$, $f(x_{i+1}, y_{j+1})$, respectively; $\sigma_{f_1}^2$, $\sigma_{f_2}^2$, $\sigma_{f_3}^2$, $\sigma_{f_4}^2$ are variances of $f(x_i, y_j)$, $f(x_i, y_{j+1})$, $f(x_{i+1}, y_j)$, $f(x_{i+1}, y_{j+1})$, respectively; $\sigma_{f_1f_2}$ is a covariance between $f(x_i, y_j)$ and $f(x_i, y_{j+1})$, $\sigma_{f_1f_3}$ is a covariance between $f(x_i, y_j)$ and $f(x_{i+1}, y_j)$, and so on.

Substitute formula (16) into formula (15), we have:

$$\begin{aligned}m_v^2=\frac{h^2k^2}{16}[&\sigma_{f_1}^2+\sigma_{f_2f_1}+\sigma_{f_3f_1}+\sigma_{f_4f_4}+\sigma_{f_1f_2}+\sigma_{f_2}^2+\sigma_{f_3f_2}+\sigma_{f_4f_2}\\&+\sigma_{f_1f_3}+\sigma_{f_2f_3}+\sigma_{f_3}^2+\sigma_{f_4f_3}+\sigma_{f_1f_4}+\sigma_{f_2f_4}+\sigma_{f_3f_4}+\sigma_{f_4}^2]\end{aligned} \tag{17}$$

Formula (17) can be simplified as:

$$m_v^2=\frac{h^2k^2}{16}\mathrm{Sum}(\boldsymbol{D}_{XX}) \tag{18}$$

where $\mathrm{Sum}(\boldsymbol{D}_{XX})$ is the sum of all elements in $\boldsymbol{D}_{XX}$. Formula (18) is a calculation result for a DEM grid unit based on TDR. For the volume of the whole DEM, its variance is:

$$m_{\mathrm{dem}}^2=\frac{h^2k^2}{16}\sum_{j=1}^{J-1}\sum_{i=1}^{I-1}\mathrm{Sum}(\boldsymbol{D}_{ij}) \tag{19}$$

where the m_{dem}^2 is the variance of the whole DEM volume; I, J are the total number of DEM grid points in X and Y directions, respectively; $\boldsymbol{D}_{ij}$ is a covariance matrix of four variables in a DEM grid at the ith row and the jth column; and $\mathrm{sum}(\boldsymbol{D}_{ij})$ is the sum of all elements in $\boldsymbol{D}_{ij}$.

2.4.2 *Error propagation based on SDR*

According to formula (4), the volume of a 3×3 window of DEM gird V_{SDR} is:

$$\begin{aligned}V_{\mathrm{SDR}}=\frac{hk}{9}(&f(x_0,y_0)+2f(x_1,y_0)+f(x_2,y_0)+2f(x_0,y_1)+4f(x_1,y_1)\\&+2f(x_2,y_1)+f(x_0,y_2)+2f(x_1,y_2)+f(x_2,y_2))\end{aligned} \tag{20}$$

Similarly, we can obtain:

$$\begin{aligned}m_{v_i}^2=\frac{h^2k^2}{81}(&\sigma_{f_1}^2+2\sigma_{f_2f_1}+\sigma_{f_3f_1}+2\sigma_{f_4f_1}+4\sigma_{f_5f_1}+2\sigma_{f_6f_1}+\sigma_{f_7f_1}+2\sigma_{f_8f_1}+\sigma_{f_9f_1}+\\&2\sigma_{f_1f_2}+4\sigma_{f_2}^2+2\sigma_{f_3f_2}+4\sigma_{f_4f_2}+8\sigma_{f_5f_2}+4\sigma_{f_6f_2}+2\sigma_{f_7f_2}+4\sigma_{f_8f_2}+2\sigma_{f_9f_2}+\\&\sigma_{f_1f_3}+2\sigma_{f_2f_3}+\sigma_{f_3}^2+2\sigma_{f_4f_3}+4\sigma_{f_5f_3}+2\sigma_{f_6f_3}+\sigma_{f_7f_3}+2\sigma_{f_8f_3}+\sigma_{f_9f_3}+\\&2\sigma_{f_1f_4}+4\sigma_{f_2f_4}+2\sigma_{f_3f_4}+4\sigma_{f_4}^2+8\sigma_{f_5f_4}+4\sigma_{f_6f_4}+2\sigma_{f_7f_4}+4\sigma_{f_8f_4}+2\sigma_{f_9f_4}+\\&4\sigma_{f_1f_5}+8\sigma_{f_2f_5}+4\sigma_{f_3f_5}+8\sigma_{f_4f_5}+16\sigma_{f_5}^2+8\sigma_{f_6f_5}+4\sigma_{f_7f_5}+8\sigma_{f_8f_5}+4\sigma_{f_9f_5}+\\&2\sigma_{f_1f_6}+4\sigma_{f_2f_6}+2\sigma_{f_3f_6}+4\sigma_{f_4f_6}+8\sigma_{f_5f_6}+4\sigma_{f_6}^2+2\sigma_{f_7f_6}+4\sigma_{f_8f_6}+2\sigma_{f_9f_6}+\\&\sigma_{f_1f_7}+2\sigma_{f_2f_7}+\sigma_{f_3f_7}+2\sigma_{f_4f_7}+4\sigma_{f_5f_7}+2\sigma_{f_6f_7}+\sigma_{f_7}^2+2\sigma_{f_8f_7}+\sigma_{f_9f_7}+\\&2\sigma_{f_1f_8}+4\sigma_{f_2f_8}+2\sigma_{f_3f_8}+4\sigma_{f_4f_8}+8\sigma_{f_5f_8}+4\sigma_{f_6f_8}+2\sigma_{f_7f_8}+4\sigma_{f_8}^2+2\sigma_{f_9f_8}+\\&\sigma_{f_1f_9}+2\sigma_{f_2f_9}+\sigma_{f_3f_9}+2\sigma_{f_4f_9}+4\sigma_{f_5f_9}+2\sigma_{f_6f_9}+\sigma_{f_7f_9}+2\sigma_{f_8f_9}+\sigma_{f_9}^2)\end{aligned} \tag{21}$$

where f_1~f_9 are $f(x_0, y_0)$, $f(x_1, y_0)$, $f(x_2, y_0)$, $f(x_0, y_1)$, $f(x_1, y_1)$, $f(x_2, y_1)$, $f(x_0, y_2)$, $f(x_1, y_2)$, $f(x_2, y_2)$, respectively; $\sigma_{f_1}^2 \sim \sigma_{f_9}^2$ are variances of f_1~f_9, respectively; $\sigma_{f_1 f_2}$ is a covariance between $f(x_0, y_0)$ and $f(x_1, y_0)$, $\sigma_{f_1 f_3}$ is a covariance between $f(x_0, y_0)$ and $f(x_2, y_0)$, and so on. Formula (21) is a VC for a 3×3 window based on SDR. For the volume of the whole DEM, its variance is:

$$m_{\text{dem}}^2 = \sum_{i=1}^{n} (m_{v_i}^2) \tag{22}$$

where the $m_{dem}{}^2$ is the variance of the whole DEM volume; n is the number of 3×3 window for a DEM; $m_{v_i}^2$ is the variance of the ith 3×3 window volume.

3 Experiments and analysis

In this section, we describe the experiments that were conducted for this study. These experiments were performed to clarify the relationship between VC accuracy and ME, DE and PE. Then, we discuss and analyse the results of the experiments.

3.1 *Experiment of TE and DE based on simulated DEM*

A real-world DEM surface function is often unknown, which prevents the theoretical true value of earthwork volume to be determined. Moreover, real-world DEM data have data source errors, which adds an uncertainty of estimating the accuracy of VC for DEMs. Hence, in this experiment, simulated DEMs with different resolution and terrain complexity were generated by an artificially designated mathematical surface. The main advantages of using mathematical (simulated) surface are that the theoretical true value of the earthwork volume can be obtained to easily estimate the accuracy and eliminate the interference of data source errors. Based on previous studies (Zhou and Liu 2004, Zhou et al. 2006, Shi and Tian 2006), a Gauss synthetic surface function was used to generate a stimulated DEM at a different resolution and terrain complexity. The Gauss synthetic surface function is given by

$$z = A\left[1-\left(\frac{x}{M}\right)^2\right]e^{-\left(\frac{x}{M}\right)^2-\left(\frac{y}{N}+1\right)^2} - B\left[0.2\left(\frac{x}{M}\right)-\left(\frac{x}{M}\right)^3-\left(\frac{y}{N}\right)^5\right]e^{-\left(\frac{x}{M}\right)^2-\left(\frac{y}{N}\right)^2} - Ce^{-\left(\left(\frac{x}{M}\right)+1\right)^2-\left(\frac{y}{N}\right)^2} \tag{23}$$

where A, B and C are parameters that determine surface relief, and M and N are the parameters that control the spatial extent of the surface (Liu 2001).

First, we use MATLAB 2013 to generate several simulated DEMs based on equation (23). For equation (23), two major steps are employed to generate a simulated DEM: a) constructing the network of elevation nodes; b) simulating DEM surfaces with different levels of complexity (Shi et al. 2005). In section 2.1, the network of elevation nodes was defined by (i, j, $z(i, j)$) (i = 1, 2, 3…, I; j = 1, 2, 3,…, J). Thus, if $x = i$, $y = j$ and $z = z(i, j)$, the network of elevation nodes can be easily constructed. The DEM surfaces at different levels of complexity can be simulated by changing the five parameters A, B, C, M, and N in equation (23). In this study, we let $a = c$ = -500 and $b = d$ = 500; thus, the interval [a, b] and the interval [c, d] are [-500, 500], and we establish $M = N$ = 250. The values of A, B, C are listed in Table 1. Figure 3 shows the surfaces of the six simulated DEMs, which represent six different terrain types. Assume that the sampling resolution is defined by the interval sampling; e.g., because (b-a)/100 = (500-(-500))/100=10, the sampling resolution is 10.

Table 1. Values of A, B and C

surface	A	B	C
G1	3	10	1/3
G2	30	100	3

G3	60	200	6
G4	90	300	9
G5	120	400	12
G6	150	500	24

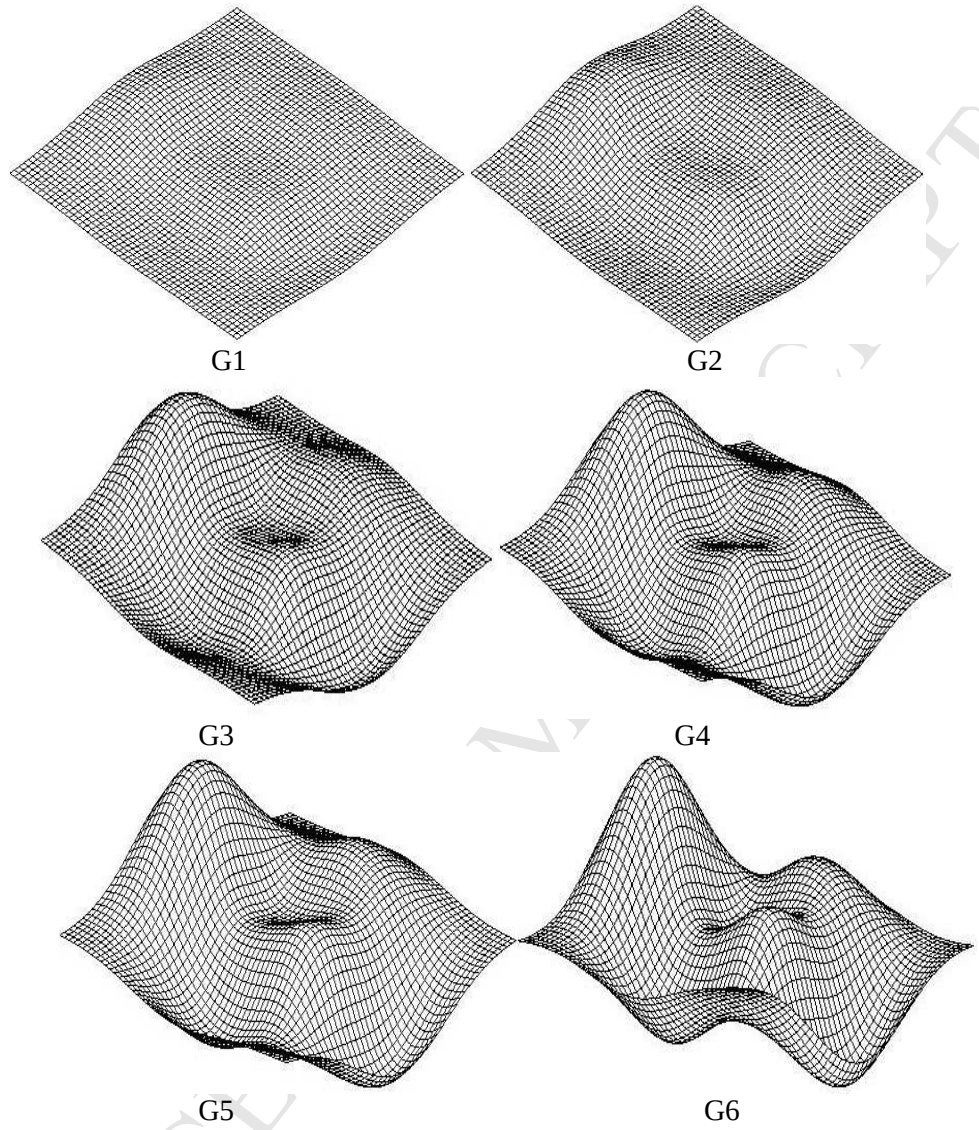

Figure 3. Surfaces of simulated DEMs with different levels of terrain complexity

Then, we use TDR and SDR to conduct VC experiments based on the six simulated DEMs. In our experiments, the fluctuation ranges of the TE and absolute error (the absolute value of the difference between the calculation value and the theoretical true value, AE) were quantified. For each simulated DEM with one level of terrain complexity, the TE and AE was counted at ten types of resolution. Based on the quantized values of TE and AE, by comparison and analysis, the relationship between MEs and VC accuracy and the relationship between DEs and VC accuracy can be reflected. The uncertainty of VCs based on a regular grid DEM can be modelled and analysed. These experiments are performed in MATLAB 2013. As the terrain surface function of simulated DEM is known, the theoretical true value of the earthwork volume can be calculated by the function “integral2” in MATLAB 2013. In the experiments, to simulate VC in the real world, integral value is calculated by formula (2) or (4) for TDR and SDR respectively; TE, namely modelling error, is calculated by formula (3) or (5) for TDR and SDR respectively; confidence intervals (i.e. measurement uncertainty) are

calculated by formula (11); and AE is calculated by formula (12). All the above mentioned methods are based on numerical calculation that is specifically designed to deal with realistic computing (e.g. discrete data) in the real world.

The experimental results are shown in Tables 2 and 3.

Table 2. Experimental results of simulated DEM G1~ G6. Sampling resolution (SR), absolute error based on TDR (AE_{TDR}), truncation error based on TDR (TE_{TDR}), absolute error based on SDR (AE_{SDR}) and truncation error based on SDR (TE_{SDR}).

DEM	SR	AE_{TDR}	TE_{TDR}	AE_{SDR}	TE_{SDR}
G1	10	0.6786	6974.6631	0.000279	14.078801
	5	0.1695	1752.1390	0.000005	3.312620
	4	0.1085	1121.8847	0.000017	2.148854
	2.5	0.0423	438.5755	0.000024	0.859674
	2	0.0271	280.7383	0.000025	0.554935
	1	0.0068	70.1976	0.000025	0.141207
	0.5	0.0017	17.5505	0.000025	0.035620
	0.4	0.0011	11.2324	0.000025	0.022838
	0.25	0.0004	4.3877	0.000025	0.008945
	0.2	0.0002	2.8081	0.000025	0.005730

DEM	SR	AE_{TDR}	TE_{TDR}	AE_{SDR}	TE_{SDR}
G2	10	11.0596	69655.0083	0.002739	140.450901
	5	2.7635	17498.4326	0.000054	33.061853
	4	1.7684	11204.4176	0.000170	21.448207
	2.5	0.6906	4380.2223	0.000239	8.581492
	2	0.4419	2803.8831	0.000246	5.539678
	1	0.1103	701.1220	0.000251	1.409687
	0.5	0.0274	175.2918	0.000252	0.355606
	0.4	0.0174	112.1877	0.000252	0.227998
	0.25	0.0067	43.8236	0.000252	0.089302
	0.2	0.0042	28.0472	0.000252	0.057205

DEM	SR	AE_{TDR}	TE_{TDR}	AE_{SDR}	TE_{SDR}
G3	10	22.1193	139310.0166	0.005478	280.901802
	5	5.5269	34996.8652	0.000108	66.123705
	4	3.5368	22408.8352	0.000340	42.896415
	2.5	1.3812	8760.4446	0.000478	17.162984
	2	0.8838	5607.7662	0.000493	11.079357
	1	0.2206	1402.2440	0.000503	2.819374
	0.5	0.0548	350.5835	0.000503	0.711211
	0.4	0.0349	224.3754	0.000503	0.455996
	0.25	0.0133	87.6473	0.000503	0.178605
	0.2	0.0083	56.0943	0.000504	0.114410

DEM	SR	AE_{TDR}	TE_{TDR}	AE_{SDR}	TE_{SDR}
G4	10	33.1789	208965.0249	0.008217	421.352704
	5	8.2904	52495.2977	0.000162	99.185558
	4	5.3053	33613.2528	0.000511	64.344622
	2.5	2.0718	13140.6669	0.000717	25.744476
	2	1.3257	8411.6493	0.000739	16.619035
	1	0.3308	2103.3661	0.000753	4.229061
	0.5	0.0821	525.8753	0.000755	1.066817

	0.4	0.0523	336.5630	0.000754	0.683993
	0.25	0.0200	131.4709	0.000754	0.267907
	0.2	0.0125	84.1415	0.000756	0.171615

DEM	SR	AE_{TDR}	TE_{TDR}	AE_{SDR}	TE_{SDR}
G5	10	44.2386	278620.0333	0.010956	561.803605
	5	11.0538	69993.7303	0.000216	132.247410
	4	7.0737	44817.6704	0.000681	85.792830
	2.5	2.7624	17520.8891	0.000956	34.325967
	2	1.7675	11215.5325	0.000986	22.158714
	1	0.4411	2804.4881	0.001005	5.638748
	0.5	0.1095	701.1670	0.001006	1.422423
	0.4	0.0697	448.7507	0.001006	0.911991
	0.25	0.0266	175.2945	0.001007	0.357210
	0.2	0.0167	112.1887	0.001007	0.228820

DEM	SR	AE_{TDR}	TE_{TDR}	AE_{SDR}	TE_{SDR}
G6	10	60.0948	350748.8441	0.015019	711.356416
	5	15.0311	88112.0125	0.000169	167.046544
	4	9.6209	56419.7620	0.000797	108.330098
	2.5	3.7591	22054.8964	0.001170	43.319487
	2	2.4063	14117.6624	0.001210	27.959410
	1	0.6025	3530.0906	0.001236	7.112758
	0.5	0.1516	882.5786	0.001238	1.794002
	0.4	0.0974	564.8533	0.001237	1.150199
	0.25	0.0388	220.6473	0.001237	0.450494
	0.2	0.0253	141.2145	0.001236	0.288572

3.2 *Experiment of error propagation in VC*

The basic idea of the PE calculation experiment is to add random error to the DEM based on Monte-Carlo simulation method and spatial characteristics (WECHSLER 1999; WECHSLER and Kroll 2006); First, add random error that obeys a normal distribution $N\sim(0,\sigma)$ to the simulated DEM in elevation values (z) or plane coordinates (x, y); second, use the neighbourhood correlation to process the random elevation error according to the Wechsler (1999)'s study with spatial autocorrelation. Exactly, the geostatistical software GS+ is used to fit the error autocorrelation model to determine the error and covariance of the grid point z or (x, y). Finally, the AE and standard deviation (SD) of the volume are calculated after adding random error by Formula (19) and (22).

According to the above experimental procedure, the error propagation experiment results are shown in Tables 3~4 and Figure 6.

Table 3. Experimental results of plane (x, y) error propagation. Coordinate SD (CSD), volume SD based on TDR (VSD_{TDR}), volume SD based on SDR (VSD_{SDR}) and sampling resolution (SR)

DEM	CSD		SR					
			20		10		5	
	x	y	VSD_{TDR}	VSD_{SDR}	VSD_{TDR}	VSD_{SDR}	VSD_{TDR}	VSD_{SDR}
G1	0.01	0.01	1.4366	1.2002	0.6482	0.5386	0.3290	0.2782
	0.05	0.05	5.8471	4.3787	3.1615	2.6270	1.5945	1.3482
	0.1	0.1	19.3893	9.2078	6.4823	5.3683	3.2902	2.7118

	0.6	0.6	71.8667	55.2100	38.1888	31.6203	19.5400	16.5213
G2	0.01	0.01	19.3893	16.1984	6.4823	5.3865	3.2902	2.7819
	0.05	0.05	59.1658	4.3787	30.8046	2.6270	15.7180	1.3482
	0.1	0.1	120.5802	92.4636	64.8350	53.6833	32.1425	27.1768
	0.6	0.6	720.7777	553.7209	366.077	285.7849	193.3200	163.4545
G3	0.01	0.01	27.4206	22.9080	13.1500	10.9270	6.7022	5.6668
	0.05	0.05	117.3174	88.0720	60.3120	47.4633	31.7912	26.8798
	0.1	0.1	267.2634	223.2796	129.3389	107.0923	64.1100	54.2058
	0.6	0.6	1440.5012	1106.6321	315.4574	261.1981	386.4658	326.7616
G4	0.01	0.01	43.3558	36.2207	18.5969	15.4532	9.4783	8.0140
	0.05	0.05	176.1841	132.2640	90.2493	71.0228	47.8630	40.4688
	0.1	0.1	360.0621	276.1036	194.2845	160.8671	96.1942	81.3334
	0.6	0.6	2160.2244	1659.5430	1100.2888	858.9613	579.6502	490.1015
G5	0.01	0.01	58.1680	48.5952	26.3000	21.8541	13.4043	11.3335
	0.05	0.05	233.5614	174.9061	126.1304	104.8086	63.7587	53.9088
	0.1	0.1	534.5267	446.5591	259.0091	214.4591	128.220	108.4116
	0.6	0.6	2883.1106	2783.1382	1538.7436	1597.6655	773.5125	820.2141
G6	0.01	0.01	72.5482	60.6089	32.2108	26.7657	16.4169	13.8807
	0.05	0.05	293.8503	4.3787	158.3471	2.6270	74.9325	1.3482
	0.1	0.1	601.8956	461.5468	325.6274	269.6188	160.9916	136.1204
	0.6	0.6	3622.8065	2214.8838	1929.5524	1274.0766	970.0793	654.0144

Table 4. Experimental results of elevation (z) error propagation. Volume SD based on TDR (VSD_{TDR}), volume SD based on SDR (VSD_{SDR}) and sampling resolution (SR).

DEM	ESD	SR					
		20		10		5	
		VSD_{TDR}	VSD_{SDR}	VSD_{TDR}	VSD_{SDR}	VSD_{TDR}	VSD_{SDR}
G1~G6	0.01	60.8342	50.1169	28.5340	21.5711	15.0834	12.1784
	0.05	263.5458	196.3453	150.7932	123.8077	76.2298	61.9079
	0.1	593.6502	439.8610	326.9756	271.7772	154.1529	127.6383
	0.6	3271.6401	2402.6416	1935.8628	1609.0600	930.8013	775.9418

3.3 ***Results and Discussion***

3.3.1 *Results and Discussion of TE and DE*

Table 2 lists the integral results by the TDR based on the six simulated DEMs with different levels of terrain complexity at different resolutions. Table 2 and figure 4 indicate that an increase in the resolution causes a gradual reduction in the AE for different types of terrain. This indicates that an improvement in resolution significantly improves the VC accuracy of TDR for different types of terrain. For the same DEM resolution, the AE for a steep area is higher than the AE for a flat area. When the DEM resolution is not the same, the AE for a steep area may remain higher than the AE for a flat area, e.g., comparing the DEM G6 to DEM G1, the AE of G6 at a resolution of 0.2 is higher than the AE of G1 at a resolution of 1.

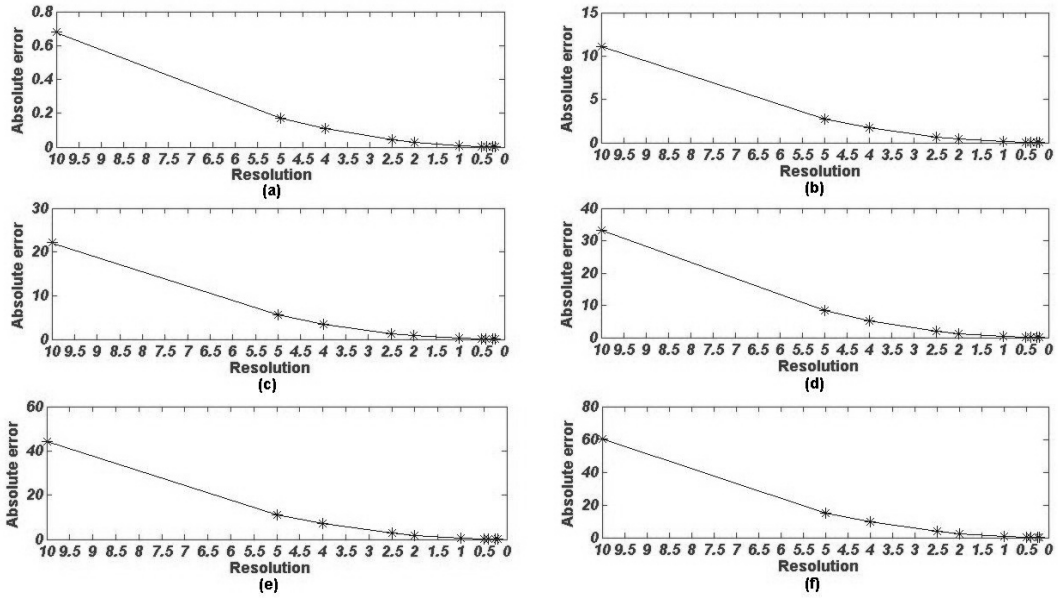

Figure 4. Relationships between absolute error and resolution based on TDR: (a)~(f) corresponds to G1~G6 (terrain complexity).

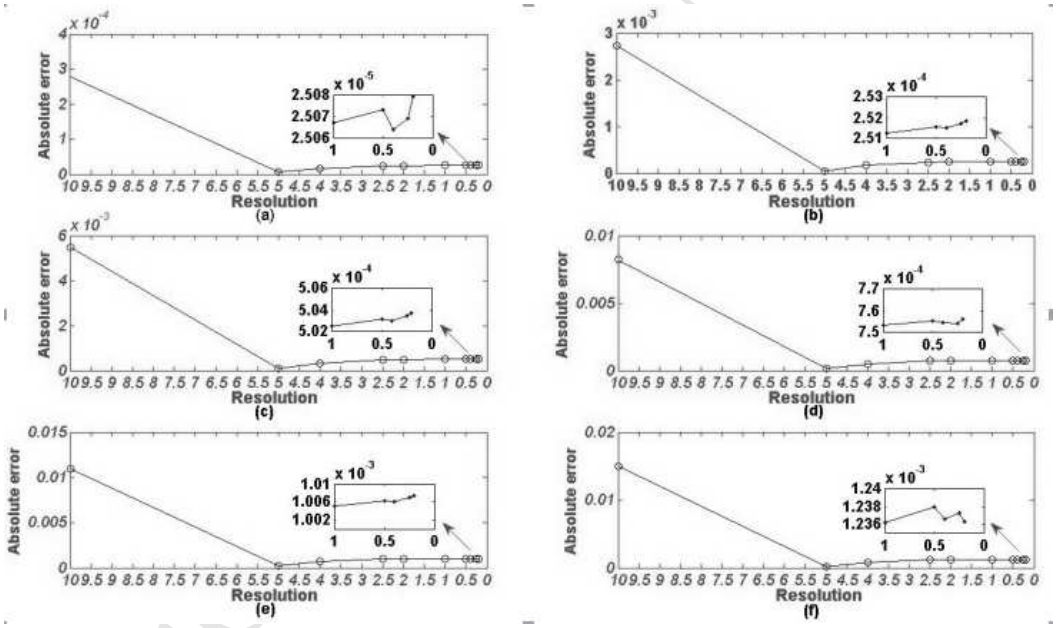

Figure 5. Relationships between absolute error and resolution based on SDR: (a)~(f) corresponds to G1~G6 (terrain complexity).

Table 2 also lists the experimental results obtained by the SDR based on the six simulated DEMs with different levels of terrain complexity at different resolutions. When the sampling resolution changes from 10 to 5, the reduction rate of AE_{SDR} is more than 90% under any different terrain complexity from G1~G5. This finding indicates that an improvement in sampling resolution causes a significant improvement in the VC accuracy of SDR for different types of terrain. As shown in figure 5, although the polylines between a sampling resolution of 5 and a sampling resolution of 0.2 seem smooth, the polylines between a sampling resolution of 5 and a sampling resolution of 0.2 exhibit fluctuations with a slight

upward trend. These results illustrate that a higher DEM resolution does not always produce better calculation results and that a fluctuation exists; e.g., in our experiment, the optimal resolution for VCs is five for the condition of DEM G2. For this phenomenon, an insufficiently small step size may cause over parameterization problem, which causes surface distortion of a DEM a decrease in the accuracy of the volume integral.

The comparison of the experimental results by TDR and SDR indicates that the maximum AE and maximum TE for TDR are approximately 60.1 and 350748, respectively. The maximum AE and maximum TE for SDR are approximately 0.015 and 711, respectively. The minimum AE and minimum TE for TDR are approximately 0.00025 and 2.8, respectively. The minimum AE and minimum TE is approximately 0.5×10^{-5} and 0.0057, respectively. For the same conditions, the VC accuracy of TDR is always less than the VC accuracy of SDR; namely, the AEs of SDR are always less than the AEs of TDR for the same conditions. The trapezoidal rule has a degree of precision of one to enable the plane to fit the DEM surface for an integral. Simpson's rule has a degree of precision of three to enable the quadratic surface to fit the DEM surface for an integral, which may cause the previously mentioned over parameterization problem.

Comparing in Table 2, an improvement in resolution causes a distinct downward trend in the TEs of TDR and SDR and a decreased rate of decline. This finding is due to the decrease in the step sizes h and k. According to equations (2) and (4), when the constant term (i.e., $(b-a)(d-c)$) does not change and the change in the maximum values of the partial derivatives is minimal, both step sizes (h and k) and partial derivatives determine the change in the TE. We also note that the value of the TE for TDR is too large for some resolutions and the change in the TE for TDR is substantially larger than the change in SDR. A comparison of the formulas of TE of TDR (i.e., equation (2)) with SDR (i.e., equation (4)) indicates that (1) $(b-a)(d-c)/12 > (b-a)(d-c)/180$; (2) the second-order partial derivatives >> the fourth-order partial derivatives; and (3) despite h^2 (or k^2) ? h^4 (or k^4) (i.e., if h=1, $h^2=h^4$; if h>1, $h^2<h^4$; and if h<1, $h^2>h^4$), these parameters are offset by the corresponding higher-order derivatives.

If AE is divided by integral value (i.e., AE/IV), which can be regarded as relative error, we discover that the relative errors are generally very small and usually account for less than 10^{-5} and less than 10^{-8} of the total volume for TDR and SDR, respectively. Although relative errors are generally very small, AEs cannot be disregarded in practice. Improving the accuracy of the VCs is the overarching goal of this study. Although we hope to be able to reduce uncertainty by investigating it, sometimes uncertainty research cannot be used to reduce uncertainty, e.g. a) just like playing dice, we can gain the knowledge on its probability, but we cannot use it to improve hit rate on anyone number of dots (pips) from 1 to 6; and b) random error in observation cannot be eliminated by any methods etc. But, discovering a law for improving VCs is still significant. Actually, uncertainty research can be used to inform practitioners about best practices to minimize uncertainty

Comparing the value of TE with absolute value, we determine that all AE values are within the range of the TE, which verifies the validity of the ME estimation. For SDR or TDR, the degree of uncertainty (i.e., variant range) of the TE all substantially larger than the degree of uncertainty of the AE values. This finding is attributed to two main reasons: (1) the constant terms (a, b, c, d, h and k), in both equations (2) and (4) are too large, e.g., $(b-a)(d-c) = 10^8$; and (2) the maximum values of the partial derivatives cannot be accurately estimated with the variant resolution.

3.3.2 *Results and Discussion of PE*

By comparing figure 6 (a)~(f), we can find out that:

1) With random errors generated for DEM, whether TDR or SDR, the AE of VCs doesn't increase with the increasing of terrain complexity. The reason is that the added random error obeys a normal distribution with mathematical expectation 0.

According to the equations (2) and (4), at the time of integral operation the random errors can cancel each other, resulting in AE of VCs around zero. With the ESD increasing, the magnitude of the fluctuation increases. The reason for this fluctuation is that the error added to the original error-free DEM is randomly generated without considering the spatial structure;

2) With DEM resolution improved, whether TDR or SDR, in different terrain complexity, the range of AE decreases. For example, the range of the blue dot line from figure 6 (*a*)~(*f*) is smaller than the green dot line, and the range of the red dot line is smaller than the blue dot line.

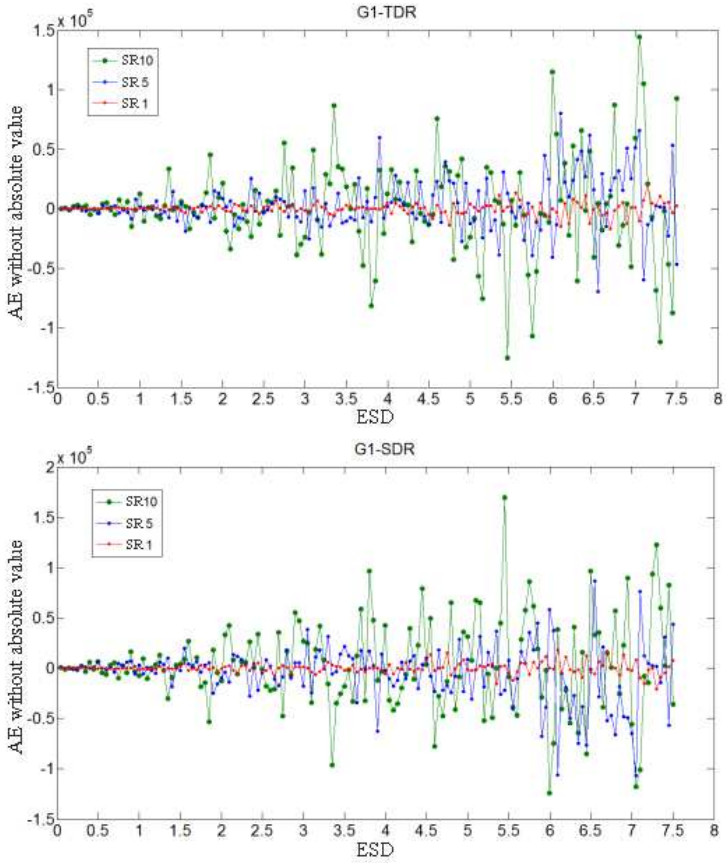

(*a*)

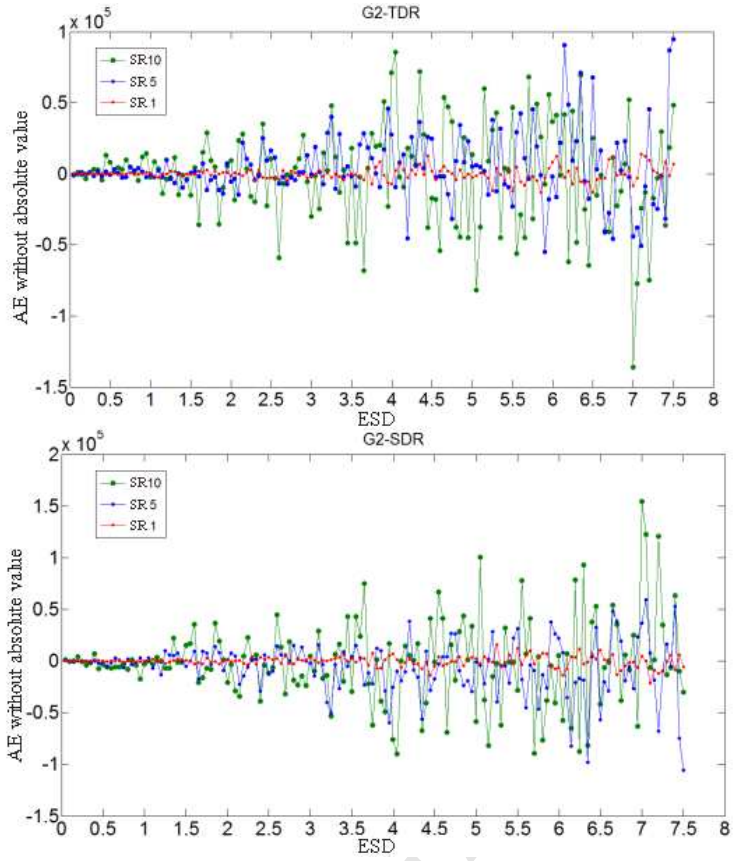
G2-TDR
x 10^5
SR10
SR5
SR1
AE without absolute value
ESD
G2-SDR
x 10^5
SR10
SR5
SR1
AE without absolute value
ESD

(*b*)

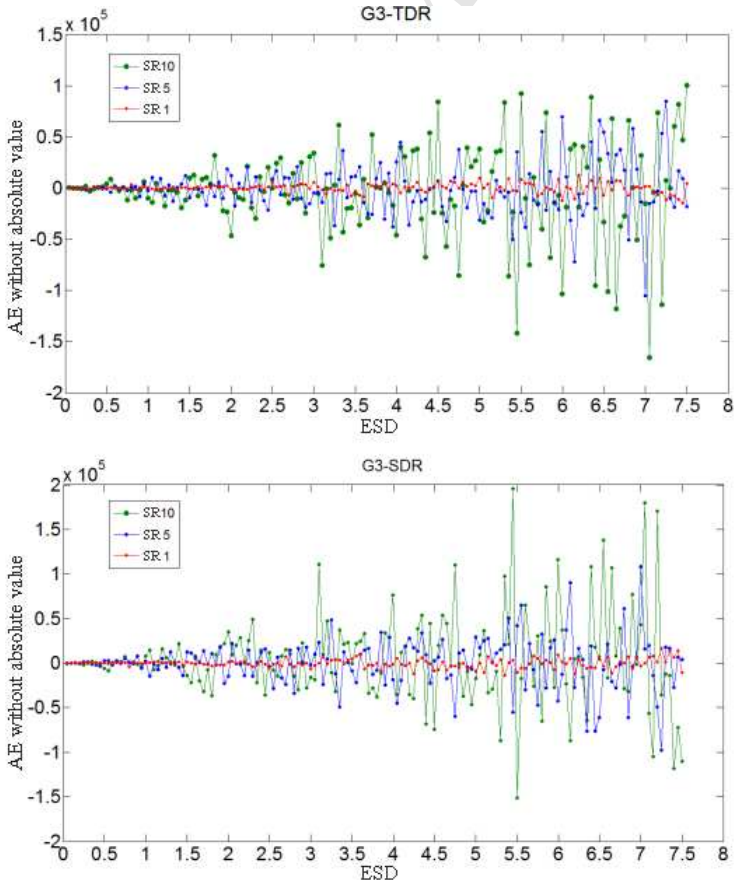
G3-TDR
x 10^5
SR10
SR5
SR1
AE without absolute value
ESD
G3-SDR
x 10^5
SR10
SR5
SR1
AE without absolute value
ESD

(*c*)

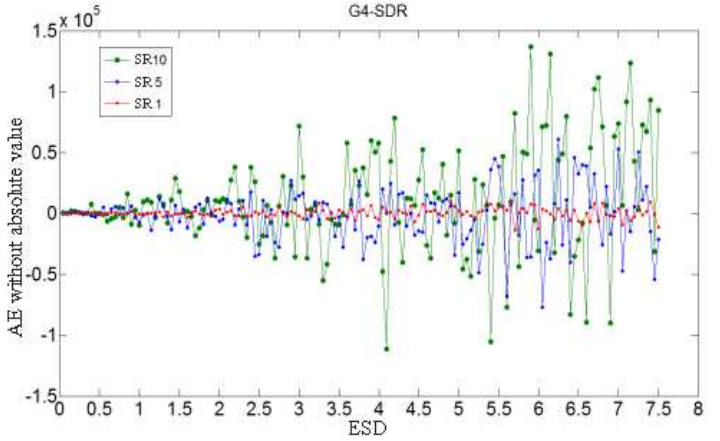
G4-SDR
x 10^5
SR10
SR5
SR1
AE without absolute value
ESD

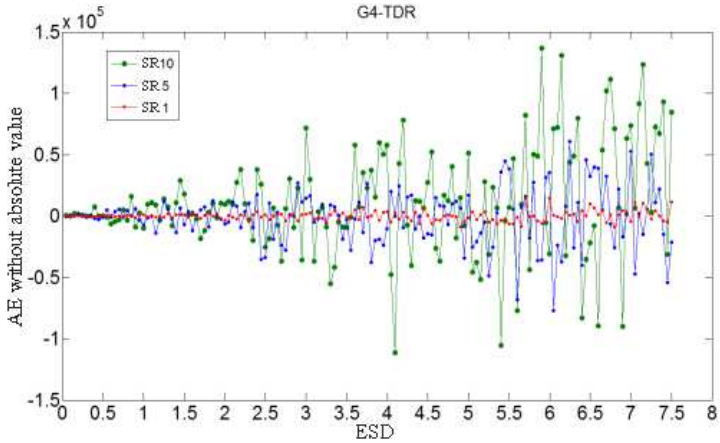
G4-TDR
x 10^5
SR10
SR5
SR1
AE without absolute value
ESD

(*d*)

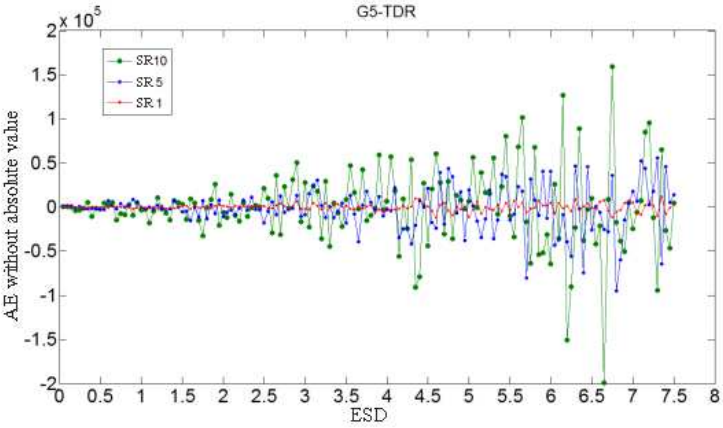
G5-TDR
x 10^5
SR10
SR5
SR1
AE without absolute value
ESD

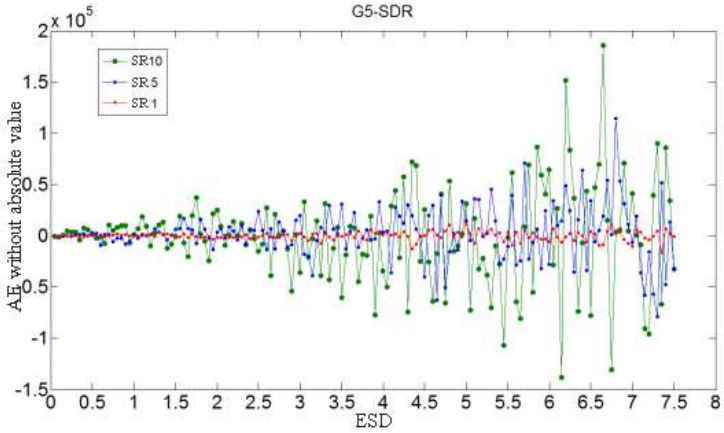
G5-SDR
x 10^5
SR10
SR5
SR1
AE without absolute value
ESD

(*e*)

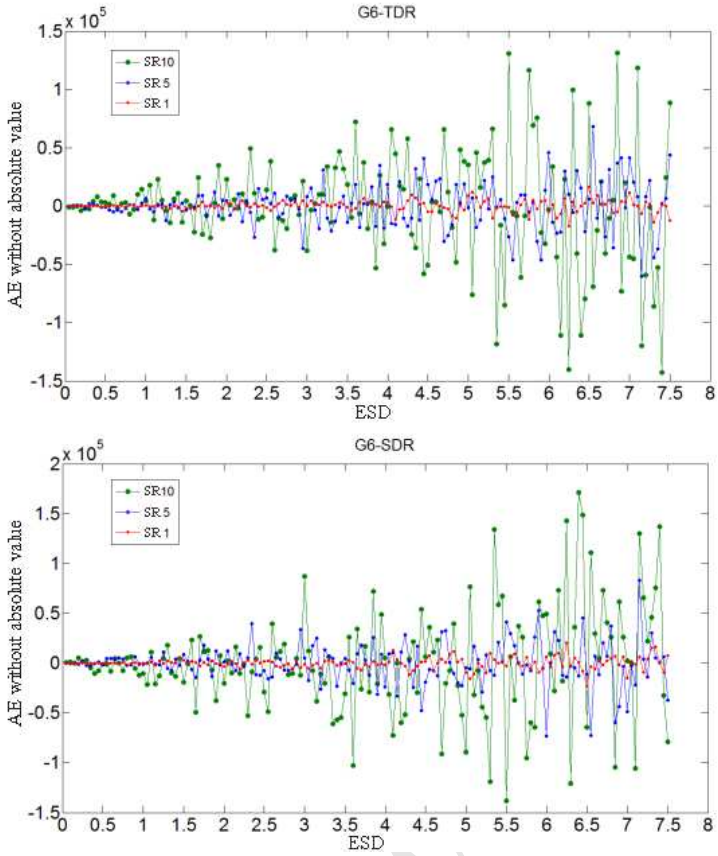

(*f*)

Figure 6. Relationships between AE without absolute value and elevation SD (ESD) in DEM G1~G6 (corresponding (*a*)~(*f*)) volume calculations using TDR and SDR at different sampling resolution (SR).

Table 3 lists experimental results of coordinate error propagation based on TDR and SDR. The comparison of the experimental results by TDR and SDR indicates that:

1) In VC, an improvement of terrain complexity causes an improvement of the VSD, and an improvement of DEM resolution reduces the VSD. These results are caused by two reasons: first, with the terrain complexity increasing, the elevation error caused by plane (*x*, *y*) error increases, so the VSD in table 3 increases; second, the size of the VSD depends on the size of the DEM resolution and the covariance between the DEM grid points according to formula (19) and formula (22);
2) For the same coordinate error, the VSD caused by the propagation of TDR is larger than that of SDR. Because the accuracy of VC based on TDR method is lower than that of SDR method;
3) Whether TDR or SDR, the AE of VC is inconsistent with the change of VSD in the case of DEM with coordinate error. Because the SD is relative error and there is a fundamental difference between the relative and AE.

Table 4 lists experimental results of elevation error propagation based on the TDR and SDR. The comparison of the experimental results by TDR and SDR indicates that:

1) In VC, whether TDR or SDR, an improvement of DEM resolution causes an improvement of the VSD, but an improvement of terrain complexity does not influence the VSD. The DEM with low terrain complexity has the same VSD as the DEM with high terrain complexity. According to formula (19) and formula (22), the VSD is only affected by DEM resolution and elevation covariance of grid points;
2) For the same elevation error, an improvement of DEM resolution reduces the AE of

VC for both TDR and SDR. With the terrain complexity increasing, the AE based on TDR gradually becomes larger, and the range of variation is large. The AE based on SDR becomes larger with slight fluctuation, but the range of variation is small. When the elevation error is small, the VSD of TDR is larger than SDR; and when the elevation error becomes larger, the AE of SDR is smaller than TDR. That is because the accuracy of VC based on TDR method is lower than that of SDR method. However, the stability of VC based on SDR is less than that of TDR, and SDR is more sensitive to elevation error.

4 Conclusions and future work

In this study, the uncertainty modelling and analysis of VCs based on a regular grid DEM was investigated using a comparative analysis of the changes in TE and AE for the simulated DEM with different levels of resolution and complexity. According to the analysis of the experiment results, we obtain the following conclusions:

(a) For the situation without DEM errors, the DEM resolution and terrain complexity affect the accuracy of the VCs based on the regular grid DEM. However, the accuracy of the VCs is more sensitive to the level of terrain complexity;

(b) Although the sensitivity of a DEM resolution is relatively lower than the terrain complexity, an increase in the resolution of the DEM, the accuracy of the VC based on regular grid DEM still be improved significantly. However, we must note that that for SDR, it is not the higher the resolution, the better the accuracy. That is, under the condition of terrain complexity G1 and resolution 5, the minimum AE is obtained. Please note that improving the resolution of a DEM may not be able to improve the accuracy of the VCs;

(c) The accuracy of the VCs based on SDR is unstable due to the fluctuation. If an ultrahigh resolution DEM is constructed in the future, a stable TDR may be a suitable choice for calculating the volume based on a regular grid DEM. When the accuracy can satisfy the requirements, TDR can simplify the calculations and reduce runtime;

(d) For the same conditions (e.g., resolution and terrain complexity), the accuracy of the SDR shows fluctuation, the accuracy of the TDR is expressed as monotonic but the convergence of SDR is faster than the TDR, the degree of uncertainty of SDR is smaller and the accuracy of SDR is better than the accuracy of the TDR. Thus, SDR is the better choice for calculating volume without considering the run time;

(e) With considering of the plane coordinate (x, y) error, results of error propagation show that both VSD and AE are related to the terrain complexity and DEM resolution;

(f) With considering of the elevation (z) error, under the same conditions, results of error propagation show that both VSD and AE are only related to the simulated z error but not related to terrain complexity;

(g) As far as the method for improving the VC accuracy is concerned, it includes, 1) acquiring the higher DEM resolution; 2) selecting SDR to calculate volume and selecting the proper resolution at the same time.

In this study, error-free simulated surfaces have been employed in the experiment. In future studies, if the simulated surfaces which include artificial setting error, are used to the experiment, and even real DEM data can be obtained, the uncertainty model of VC based on a regular grid DEM will be more deeply studied.

Acknowledgments

This study is supported by the National Natural Science Foundation of China (NSFC) (grant nos. 41771493 and 41101407); the Natural Science Foundation of Hubei Province (grant nos. 2014CFB377 and 2010CDZ005), China; Wuhan Youth Science and technology plan (Grant

No. 2016070204010137) and self-determined research funds of CCNU from the colleges' basic research and operation of MOE (grant nos. CCNU15A02001). We also are grateful for the comments and contributions of the anonymous reviewers and the members of the editorial team.

References

ARBOGAST A. F., SHORTRIDGE, A. M., & BIGSBY, M. E. 2009. Volumetric Estimates of Coastal Sand Dunes in Lower Michigan: Explaining the Geography of Dune Fields. Physical Geography, 30(6), 479-500.

CARLISLE, B. H. 2005. Modelling the spatial distribution of DEM error. Transactions in GIS, 9(4), 521-540.

GOODCHILD, M. F. 1992. Geographical information science. International Journal of Geographical Information Systems, 6(1), 31-45.

GOODCHILD, M. F. and JEANSOULIN, R., 1998. Data quality in geographic information: from error to uncertainty. Hermes Paris.

JAMES, T. D., CARBONNEAU, P. E. and LANE, S. N. 2007. Investigating the effects of DEM error in scaling analysis. Photogrammetric Engineering & Remote Sensing, 73(1), 67-78.

KERLE, N. 2002. Volume estimation of the 1998 flank collapse at Casita volcano, Nicaragua: a comparison of photogrammetric and conventional techniques. Earth Surface Processes and Landforms, 27(7), 759-772.

Lane, S. N., Westaway, R. M., & Murray Hicks, D. 2003. Estimation of erosion and deposition volumes in a large, gravel□bed, braided river using synoptic remote sensing. Earth Surface Processes and Landforms, 28(3), 249-271.

LI, D., ZHANG, J. and WU, H. 2012. Spatial data quality and beyond. International Journal of Geographical Information Science, 26(12), 2277-2290.

LI, Z., ZHU, Q. and GOLD, C., 2005, Digital Terrain Modelling: Principles and Methodology (Boca Raton: CRC Press).

LIU, X., 2001. on the accuracy of algorithm for interpreting grid-basd digtial terrain model. phd. Wuhan University.

SEFERCIK, U. G., DANA, I. 2012. Crucial Points of Interferometric Processing for dem Generation Using High Resolution SAR Data. International Archives of the Photogrammetry, Remote Sensing and Spatial Information Sciences. XXXVIII-4/W19 (4) :289-296.

SHI, W., 2009. Principles of modeling uncertainties in spatial data and spatial analyses. Boca Raton: CRC Press.

SHI, W. Z., LI, Q. Q. and ZHU, C. Q. 2005. Estimating the propagation error of DEM from higher□order interpolation algorithms. International Journal of Remote Sensing, 26(14), 3069-3084.

SHI, W. Z. and TIAN, Y. 2006. A hybrid interpolation method for the refinement of a regular grid digital elevation model. International Journal of Geographical Information Science, 20(1), 53-67.

SLATTERY, K. T., SLATTERY, D. K. and PETERSON, J. P. 2011. Road construction earthwork volume calculation using three-dimensional laser scanning. Journal of Surveying Engineering, 138(2), 96-99.

SMITH, S. D., WOOD, G. S. and GOULD, M. 2000. A new earthworks estimating methodology. Construction Management & Economics, 18(2), 219-228.

WECHSLER, S. P. 1999. Digital Elevation Model (DEM) Uncertainty: Evaluation and Effect on Topographic Parameters [EB/OL].

WECHSLER, S. P., and Kroll, C. N. 2006. Quantifying DEM Uncertainty and its Effect on Topographic Parameters. Photogrammetric Engineering & Remote Sensing, 72 (9), 1081-1090

http://ibis.geog.ubc.ca/courses/geob370/notes/uncertainty/DEM_uncertainty_wechsler_dissertation.htm

TSUTSUI, K., ROKUGAWA, S., NAKAGAWA, H., MIYAZAKI, S., CHENG, C. T., SHIRAISHI, T., & YANG, S. D. 2007. Detection and volume estimation of large-scale landslides based on elevation-change analysis using DEMs extracted from high-resolution satellite stereo imagery. IEEE transactions on geoscience and remote sensing, 45(6), 1681-1696.

WHEATON, J. M., BRASINGTON, J., DARBY, S. E., & SEAR, D. A. 2010. Accounting for uncertainty in DEMs from repeat topographic surveys: improved sediment budgets. Earth Surface Processes and Landforms, 35(2), 136-156.

WIGMORE, O. 2014. High Resolution Aerial Photogrammetry and DEM Generation in the Peruvian Andes: Evaluation of a Kite Based Platform. Association of American Geographers Meeting.

WU, L., GAO, Z. and SHI, W., 2010. Uncertainties in Geographical Information System (in Chinese). Bei Jing: Publishing House of Electronics Industry.

ZHOU, Q. and LIU, X. 2002. Error assessment of grid-based flow routing algorithms used in hydrological models. International Journal of Geographical Information Science, 16(8), 819-842.

ZHOU, Q. and LIU, X. 2004. Analysis of errors of derived slope and aspect related to DEM data properties. Computers & Geosciences, 30(4), 369-378.

ZHOU, Q., LIU, X. and SUN, Y. 2006. Terrain complexity and uncertainties in grid□based digital terrain analysis. International Journal of Geographical Information Science, 20(10), 1137-1147.

Appendix 1. Detailed derivation of trapezoidal double rule

Writing the double integral in equation (1) as

$$\iint_R f(x,y)\mathrm{d}x\mathrm{d}y = \int_a^b \left(\int_c^d f(x,y)\mathrm{d}y\right)\mathrm{d}x \tag{A1}$$

We use the composite trapezoidal rule to approximate

$$\int_c^d f(x,y)\mathrm{d}y \tag{A2}$$

Treating x as a constant.

Let $y_j = c + jk$, for each $j = 0, 1,..., m$. Then,

$$\int_c^d f(x,y)\mathrm{d}y = \frac{k}{2}\sum_{j=0}^{m}\left[f(x,y_j)+f(x,y_{j+1})\right] - \frac{(d-c)k^2}{12}\frac{\partial^2}{\partial y^2}f(x,\mu) \tag{A3}$$

For some μ in (c, d). Thus

$$\int_a^b\left(\int_c^d f(x,y)\mathrm{d}y\right)\mathrm{d}x = \frac{k}{2}\left[\sum_{j=0}^{m}\int_a^b f(x,y_j)\mathrm{d}x + \sum_{j=0}^{m}\int_a^b f(x,y_{j+1})\mathrm{d}x\right] - \frac{(d-c)k^2}{12}\int_a^b \frac{\partial^2}{\partial y^2}f(x,\mu)\mathrm{d}x \tag{A4}$$

The composite trapezoidal rule is employed in the integrals in this equation. Let $x_i = a + ih$, for each $i = 0, 1,..., n$. For each $j = 0, 1,..., m$, we have

$$\int_a^b f(x,y_j)\mathrm{d}x = \frac{h}{2}\sum_{i=0}^{n}\left[f(x_i,y_j)+f(x_{i+1},y_j)\right] - \frac{(b-a)h^2}{12}\frac{\partial^2 f}{\partial x^2}(\xi_j,y_j) \tag{A5}$$

For some ξ_j in (a, b). The resulting approximation has the form of equation (2).

The error term E_{TDR} is given by

$$E_{\mathrm{TDR}} = -\frac{(b-a)h^2}{12}\frac{k}{2}\left[\sum_{j=0}^{m}\frac{\partial^2 f}{\partial x^2}(\xi_j,y_j)+\sum_{j=0}^{m}\frac{\partial^2 f}{\partial x^2}(\xi_{j+1},y_{j+1})\right] - \frac{(d-c)k^2}{12}\int_a^b\frac{\partial^2 f}{\partial y^2}(x,\mu)\mathrm{d}x \tag{A6}$$

If $\partial^2 f/\partial x^2$ is continuous, the Intermediate Value Theorem can be repeatedly applied to show that the evaluation of the partial derivatives with respect to x can be replaced by a common value and that

$$E_{\mathrm{TDR}} = -\frac{(b-a)h^2}{12}\frac{k}{2}\left[2m\frac{\partial^2 f}{\partial x^2}(\xi,\eta)\right] - \frac{(d-c)k^2}{12}\int_a^b\frac{\partial^2 f}{\partial y^2}(x,\mu)\mathrm{d}x \tag{A7}$$

For some (ξ,η) in R. If $\partial^2 f/\partial x^2$ is also continuous, the Weighted Mean Value Theorem implies that

$$\int_a^b\frac{\partial^2 f}{\partial y^2}(x,\mu)\mathrm{d}x = (b-a)\frac{\partial^2 f}{\partial y^2}(\bar{\xi},\bar{\eta}) \tag{A8}$$

For some $(\bar{\xi},\bar{\eta})$ in R. Because $m = (d-c)/\mathrm{k}$, the error term has the form

$$E_{\mathrm{TDR}} = -\frac{(b-a)h^2}{12}\frac{k}{2}\left[2m\frac{\partial^2 f}{\partial x^2}(\xi,\eta)\right] - \frac{(b-a)(d-c)}{12}k^2\frac{\partial^2 f(\bar{\xi},\bar{\eta})}{\partial y^2} \tag{A9}$$

E_{TDR} can be simplified to equation (3).

Appendix 2. Detailed derivation of Simpson's double rule

Writing the double integral as the double integral (equation (1)) as

$$\iint_R f(x,y)\mathrm{d}x\mathrm{d}y = \int_a^b\left(\int_c^d f(x,y)dy\right)dx \tag{A10}$$

We use the Composite Simpson's rule to approximate

$$\int_c^d f(x,y)dy \tag{A11}$$

Treating x as a constant.

Let $y_j = c + jk$, for each $j = 0, 1,..., 2m$. Then,

$$\int_c^d f(x,y)\mathrm{d}y = \frac{k}{3}\left[f(x,y_0) + 2\sum_{j=1}^{m-1} f(x,y_{2j}) + 4\sum_{j=1}^{m} f(x,y_{2j-1}) + f(x,y_{2m}) \right] - \frac{(d-c)k^4}{180}\frac{\partial^4 f}{\partial y^4}(x,\mu) \tag{A12}$$

For some μ in(c, d). Thus,

$$\int_a^b \left(\int_c^d f(x,y)\mathrm{d}y\right)\mathrm{d}x = \frac{k}{3}\left[\int_a^b f(x,y_0)\mathrm{d}x + 2\int_a^b \sum_{j=1}^{m-1} f(x,y_{2j})\mathrm{d}x + 4\int_a^b \sum_{j=1}^{m} f(x,y_{2j-1})\mathrm{d}x + \int_a^b f(x,y_{2m})\mathrm{d}x \right] - \frac{(d-c)k^4}{180}\int_a^b \frac{\partial^4 f}{\partial y^4}(x,\mu)\mathrm{d}x \tag{A13}$$

Composite Simpson's rule is now employed in the integrals in this equation. Let $x_i = a + ih$, for each i = 0, 1,...,2n. For each j = 0, 1,..., 2m, we have

$$\int_a^b f(x,y_j)\mathrm{d}x = \frac{h}{3}[f(x_0,y_j) + 2\sum_{i=1}^{n-1} f(x_{2i},y_j) + 4\sum_{i=1}^{n} f(x_{2i-1},y_j) + f(x_{2n},y_j)] - \frac{(b-a)h^4}{180}\frac{\partial^4 f}{\partial x^4}(\xi_j,y_j) \tag{A14}$$

For some ξ_j in (a, b). Equation (4) can be obtained by replacing integral in equation (A13) with equation (A14)

$$\begin{aligned}\iint_R f(x,y)\mathrm{d}x\mathrm{d}y = \int_a^b\int_c^d f(x,y)\mathrm{d}y\mathrm{d}x = \frac{hk}{9}\{&[f(x_0,y_0) + 2\sum_{i=1}^{n-1} f(x_{2i},y_0) \\ &+ 4\sum_{i=1}^{n} f(x_{2i-1},y_0) + f(x_{2n},y_0)] \\ &+ 2[\sum_{j=1}^{m-1} f(x_0,y_{2j}) + 2\sum_{j=1}^{m-1}\sum_{i=1}^{n-1} f(x_{2i},y_{2j}) \\ &+ 4\sum_{j=1}^{m-1}\sum_{i=1}^{n} f(x_{2i-1},y_{2j}) + \sum_{j=1}^{m-1} f(x_{2n},y_{2j})] \\ &+ 4[\sum_{j=1}^{m} f(x_0,y_{2j-1}) + 2\sum_{j=1}^{m}\sum_{i=1}^{n-1} f(x_{2i},y_{2j-1}) \\ &+ 4\sum_{j=1}^{m}\sum_{i=1}^{n} f(x_{2i-1},y_{2j-1}) + \sum_{j=1}^{m} f(x_{2n},y_{2j-1})] \\ &+ [f(x_0,y_{2m}) + 2\sum_{i=1}^{n-1} f(x_{2i},y_{2m}) + 4\sum_{i=1}^{n} f(x_{2i-1},y_{2m}) \\ &+ f(x_{2n},y_{2m})]\} + E_{\mathrm{SDR}}\end{aligned} \tag{A15}$$

The error term E_{SDR} is given by

$$E_{\mathrm{SDR}} = \frac{-k(b-a)h^4}{540}[\frac{\partial^4 f}{\partial x^4}(\xi_0,y_0) + 2\sum_{j=1}^{m-1}\frac{\partial^4 f}{\partial x^4}(\xi_{2j},y_{2j}) + 4\sum_{j=1}^{m}\frac{\partial^4 f}{\partial x^4}(\xi_{2j-1},y_{2j-1}) + \frac{\partial^4 f}{\partial x^4}(\xi_{2m},y_{2m})] - \frac{(d-c)k^4}{180}\int_a^b \frac{\partial^4 f}{\partial y^4}(x,\mu)\mathrm{d}x \tag{A16}$$

If $\partial^4 f / \partial x^4$ are continuous, the Intermediate Value Theorem can be repeatedly applied to show that the evaluation of the partial derivatives with respect to x can be replaced by a common value and that

$$E_{\mathrm{SDR}} = \frac{-k(b-a)h^4}{540}[6m\frac{\partial^4 f}{\partial x^4}(\bar{\eta},\bar{\mu})] - \frac{(d-c)k^4}{180}\int_a^b \frac{\partial^4 f(x,\mu)}{\partial y^4}\mathrm{d}x \tag{A17}$$

For some $(\bar{\eta},\bar{\mu})$ in R. If $\partial^4 f/\partial x^4$ is also continuous, the Weighted Mean Value Theorem implies that

$$\int_a^b \frac{\partial^4 f}{\partial y^4}(x,\mu)\mathrm{d}x = (b-a)\frac{\partial^4 f}{\partial y^4}(\hat{\eta},\hat{\mu}) \tag{A18}$$

For some $(\hat{\eta},\hat{\mu})$ in R. Because m= (d−c)/2k, the error term has the form

$$E_{\mathrm{SDR}} = \frac{-k(b-a)h^4}{540}[6m\frac{\partial^4 f}{\partial x^4}(\bar{\eta},\bar{\mu})] - \frac{(b-a)(d-c)k^4}{180}(b-a)\frac{\partial^2 f}{\partial y^2}(\hat{\eta},\hat{\mu}) \tag{A19}$$

E_{SDR} can be simplified to equation (5).

surface	*A*	*B*	*C*
G1	3	10	1/3
G2	30	100	3
G3	60	200	6
G4	90	300	9
G5	120	400	12
G6	150	500	24

DEM	SR	AE_{TDR}	TE_{TDR}	AE_{SDR}	TE_{SDR}
	10	0.6786	6974.6631	0.000279	14.078801
	5	0.1695	1752.139	0.000005	3.31262
	4	0.1085	1121.8847	0.000017	2.148854
	2.5	0.0423	438.5755	0.000024	0.859674
G1	2	0.0271	280.7383	0.000025	0.554935
	1	0.0068	70.1976	0.000025	0.141207
	0.5	0.0017	17.5505	0.000025	0.03562
	0.4	0.0011	11.2324	0.000025	0.022838
	0.25	0.0004	4.3877	0.000025	0.008945
	0.2	0.0002	2.8081	0.000025	0.00573

DEM	SR	AE_{TDR}	TE_{TDR}	AE_{SDR}	TE_{SDR}
	10	11.0596	69655.01	0.002739	140.4509
	5	2.7635	17498.43	0.000054	33.06185
	4	1.7684	11204.42	0.00017	21.44821
	2.5	0.6906	4380.222	0.000239	8.581492
G2	2	0.4419	2803.883	0.000246	5.539678
	1	0.1103	701.122	0.000251	1.409687
	0.5	0.0274	175.2918	0.000252	0.355606
	0.4	0.0174	112.1877	0.000252	0.227998
	0.25	0.0067	43.8236	0.000252	0.089302
	0.2	0.0042	28.0472	0.000252	0.057205

DEM	SR	AE_{TDR}	TE_{TDR}	AE_{SDR}	TE_{SDR}
	10	22.1193	139310	0.005478	280.9018
	5	5.5269	34996.87	0.000108	66.12371
	4	3.5368	22408.84	0.00034	42.89642
	2.5	1.3812	8760.445	0.000478	17.16298
G3	2	0.8838	5607.766	0.000493	11.07936
	1	0.2206	1402.244	0.000503	2.819374
	0.5	0.0548	350.5835	0.000503	0.711211
	0.4	0.0349	224.3754	0.000503	0.455996
	0.25	0.0133	87.6473	0.000503	0.178605
	0.2	0.0083	56.0943	0.000504	0.11441

DEM	SR	AE_{TDR}	TE_{TDR}	AE_{SDR}	TE_{SDR}
	10	33.1789	208965	0.008217	421.3527
	5	8.2904	52495.3	0.000162	99.18556
	4	5.3053	33613.25	0.000511	64.34462
	2.5	2.0718	13140.67	0.000717	25.74448
G4	2	1.3257	8411.649	0.000739	16.61904
	1	0.3308	2103.366	0.000753	4.229061
	0.5	0.0821	525.8753	0.000755	1.066817
	0.4	0.0523	336.563	0.000754	0.683993
	0.25	0.02	131.4709	0.000754	0.267907
	0.2	0.0125	84.1415	0.000756	0.171615

DEM	SR	AE_{TDR}	TE_{TDR}	AE_{SDR}	TE_{SDR}

	10	44.2386	278620	0.010956	561.8036
	5	11.0538	69993.73	0.000216	132.2474
	4	7.0737	44817.67	0.000681	85.79283
	2.5	2.7624	17520.89	0.000956	34.32597
G5	2	1.7675	11215.53	0.000986	22.15871
	1	0.4411	2804.488	0.001005	5.638748
	0.5	0.1095	701.167	0.001006	1.422423
	0.4	0.0697	448.7507	0.001006	0.911991
	0.25	0.0266	175.2945	0.001007	0.35721
	0.2	0.0167	112.1887	0.001007	0.22882

DEM	SR	AE_{TDR}	TE_{TDR}	AE_{SDR}	TE_{SDR}
	10	60.0948	350748.8	0.015019	711.3564
	5	15.0311	88112.01	0.000169	167.0465
	4	9.6209	56419.76	0.000797	108.3301
	2.5	3.7591	22054.9	0.00117	43.31949
G6	2	2.4063	14117.66	0.00121	27.95941
	1	0.6025	3530.091	0.001236	7.112758
	0.5	0.1516	882.5786	0.001238	1.794002
	0.4	0.0974	564.8533	0.001237	1.150199
	0.25	0.0388	220.6473	0.001237	0.450494
	0.2	0.0253	141.2145	0.001236	0.288572

DEM	CSD		SR					
			20		10		5	
	x	*y*	VSD_{TDR}	VSD_{SDR}	VSD_{TDR}	VSD_{SDR}	VSD_{TDR}	VSD_{SDR}
G1	0.01	0.01	1.4366	1.2002	0.6482	0.5386	0.329	0.2782
	0.05	0.05	5.8471	4.3787	3.1615	2.627	1.5945	1.3482
	0.1	0.1	19.3893	9.2078	6.4823	5.3683	3.2902	2.7118
	0.6	0.6	71.8667	55.21	38.1888	31.6203	19.54	16.5213
G2	0.01	0.01	19.3893	16.1984	6.4823	5.3865	3.2902	2.7819
	0.05	0.05	59.1658	4.3787	30.8046	2.627	15.718	1.3482
	0.1	0.1	120.5802	92.4636	64.835	53.6833	32.1425	27.1768
	0.6	0.6	720.7777	553.7209	366.077	285.7849	193.32	163.4545
G3	0.01	0.01	27.4206	22.908	13.15	10.927	6.7022	5.6668
	0.05	0.05	117.3174	88.072	60.312	47.4633	31.7912	26.8798
	0.1	0.1	267.2634	223.2796	129.3389	107.0923	64.11	54.2058
	0.6	0.6	1440.5012	1106.6321	315.4574	261.1981	386.4658	326.7616
G4	0.01	0.01	43.3558	36.2207	18.5969	15.4532	9.4783	8.014
	0.05	0.05	176.1841	132.264	90.2493	71.0228	47.863	40.4688
	0.1	0.1	360.0621	276.1036	194.2845	160.8671	96.1942	81.3334
	0.6	0.6	2160.2244	1659.543	1100.2888	858.9613	579.6502	490.1015
G5	0.01	0.01	58.168	48.5952	26.3	21.8541	13.4043	11.3335
	0.05	0.05	233.5614	174.9061	126.1304	104.8086	63.7587	53.9088
	0.1	0.1	534.5267	446.5591	259.0091	214.4591	128.22	108.4116
	0.6	0.6	2883.1106	2783.1382	1538.7436	1597.6655	773.5125	820.2141
G6	0.01	0.01	72.5482	60.6089	32.2108	26.7657	16.4169	13.8807
	0.05	0.05	293.8503	4.3787	158.3471	2.627	74.9325	1.3482
	0.1	0.1	601.8956	461.5468	325.6274	269.6188	160.9916	136.1204
	0.6	0.6	3622.8065	2214.8838	1929.5524	1274.0766	970.0793	654.0144

DEM	ESD	SR					
		20		10		5	
		VSD_{TDR}	VSD_{SDR}	VSD_{TDR}	VSD_{SDR}	VSD_{TDR}	VSD_{SDR}
G1~ G6	0.01	60.8342	50.1169	28.534	21.5711	15.0834	12.1784
	0.05	263.5458	196.3453	150.7932	123.8077	76.2298	61.9079
	0.1	593.6502	439.861	326.9756	271.7772	154.1529	127.6383
	0.6	3271.6401	2402.6416	1935.8628	1609.06	930.8013	775.9418

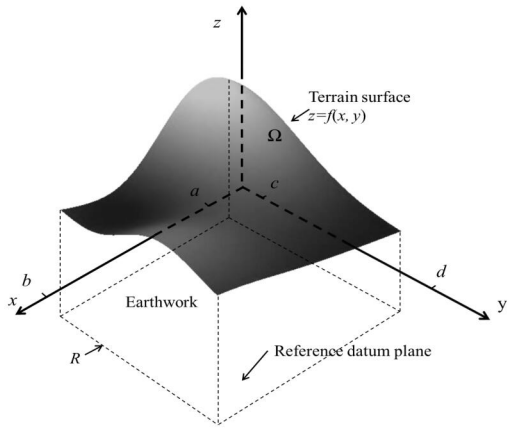

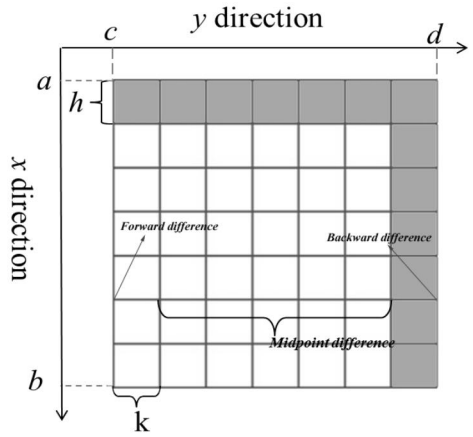

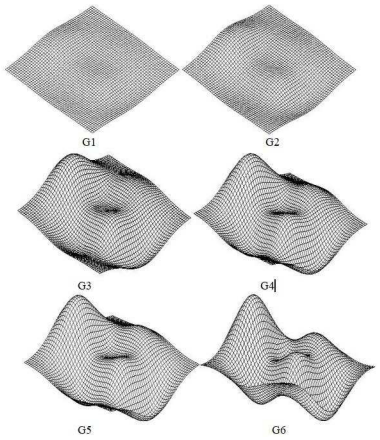

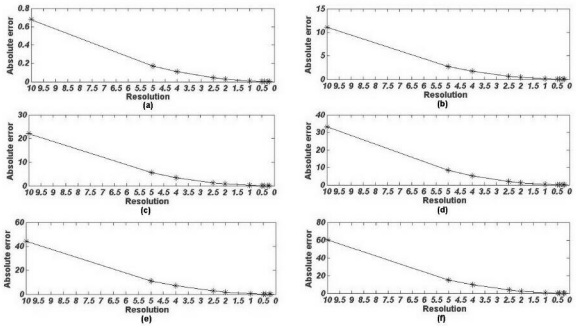

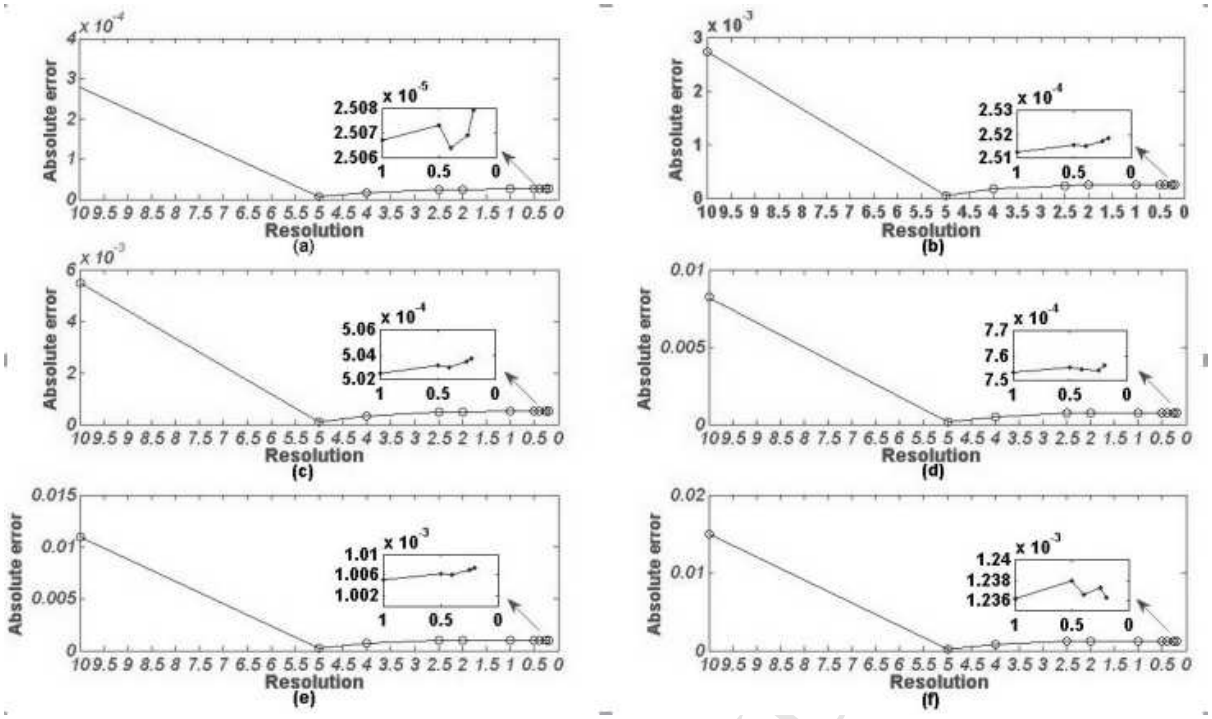

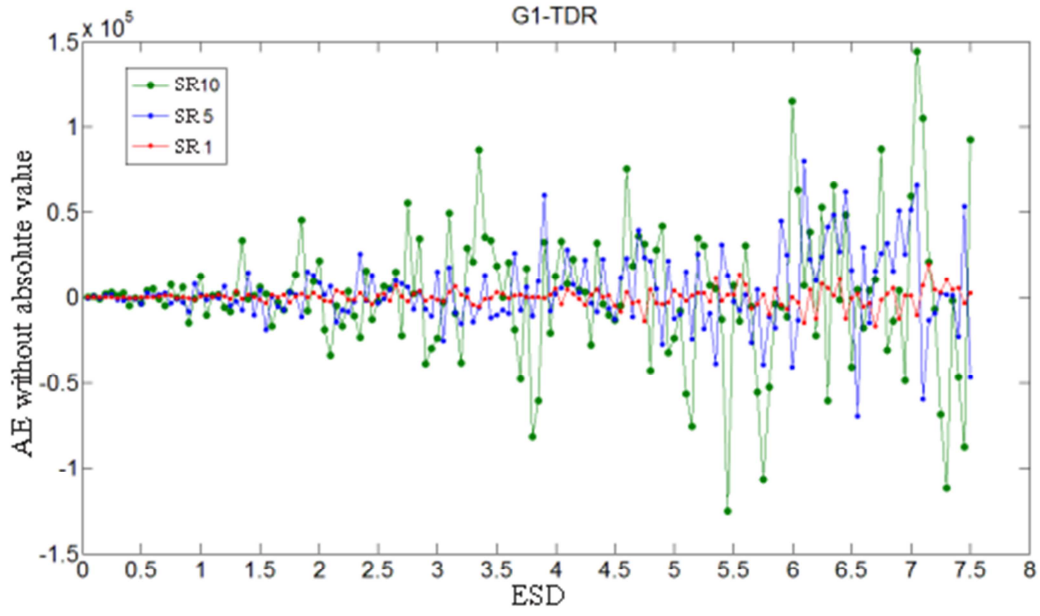
G1-TDR
x 10^5
SR10
SR5
SR1
AE without absolute value
ESD

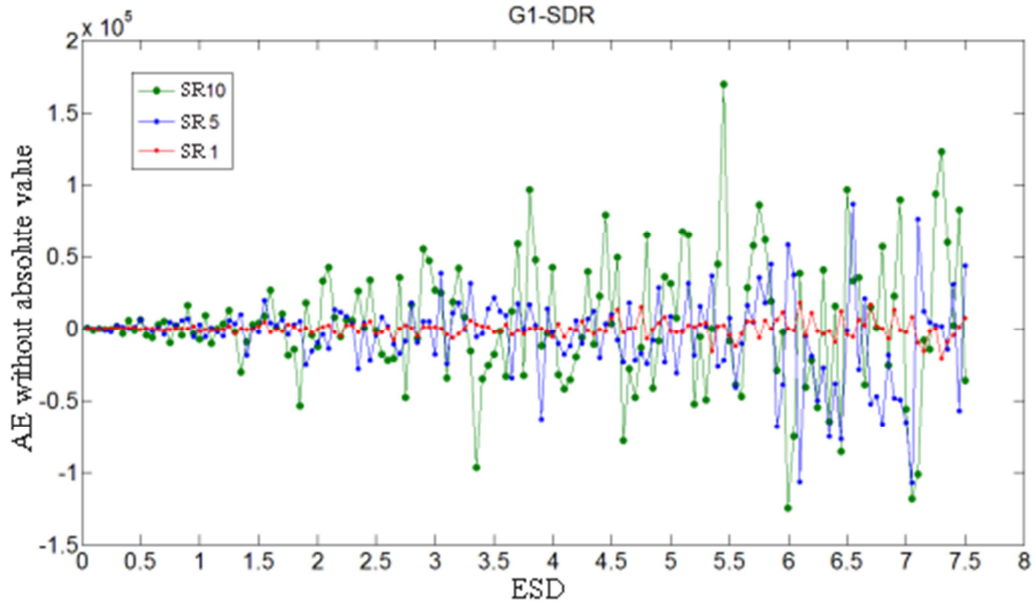
G1-SDR
x 10^5
SR10
SR5
SR1
AE without absolute value
ESD

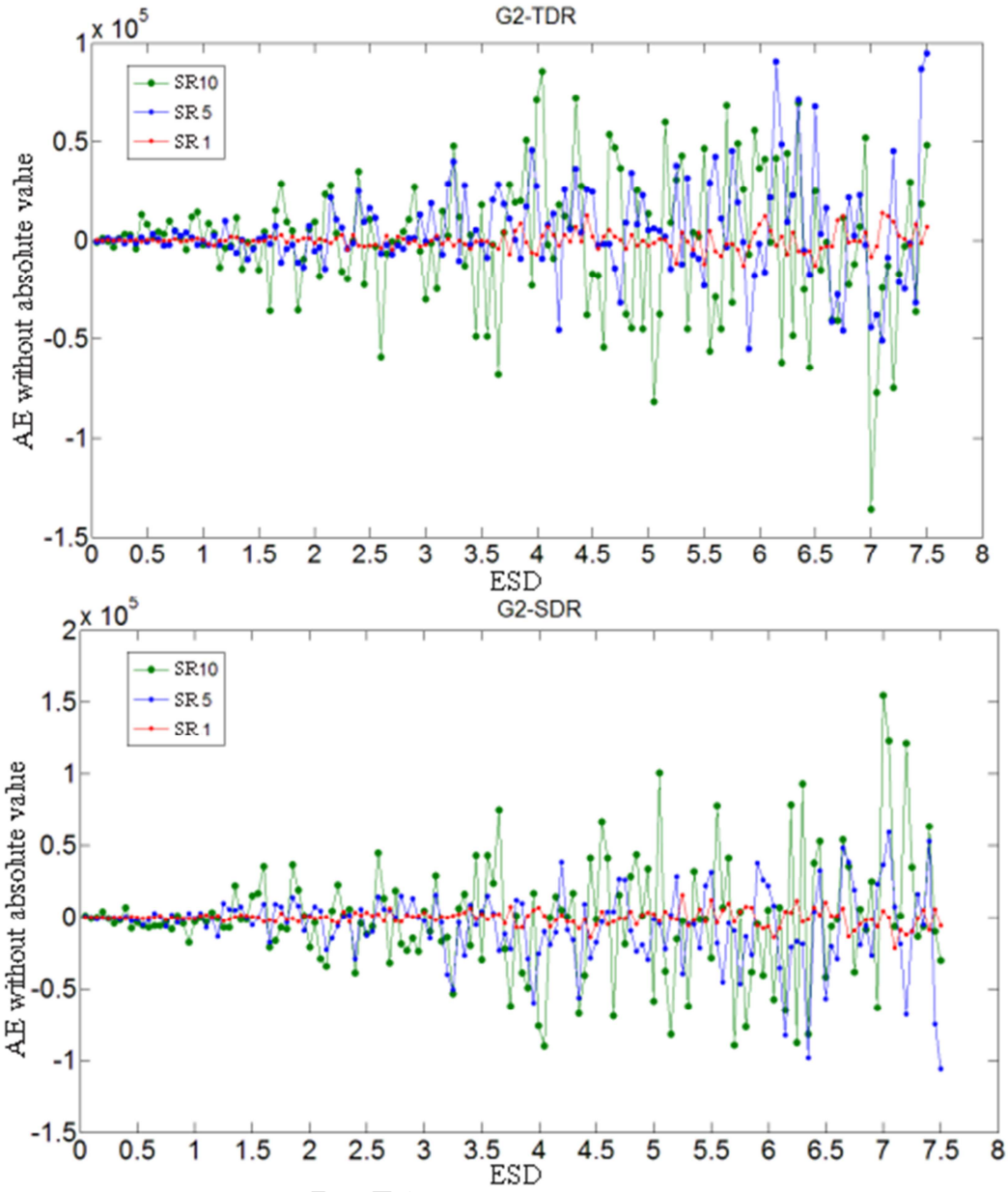
G2-TDR
x 10^5
SR10
SR5
SR1
AE without absolute value
ESD
G2-SDR
x 10^5
SR10
SR5
SR1
AE without absolute value
ESD

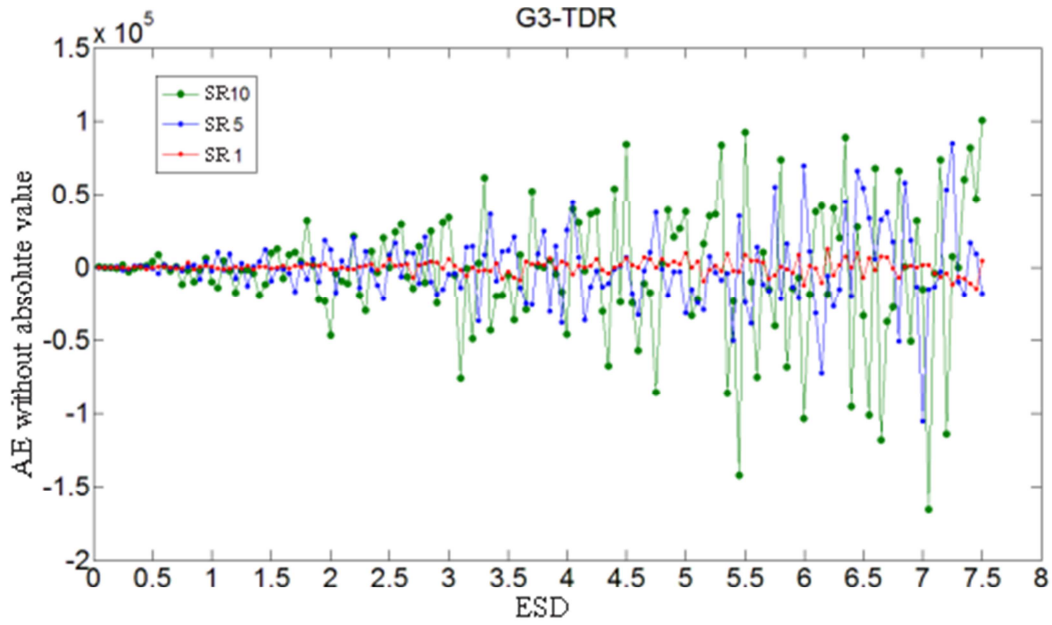
G3-TDR
x 10^5
SR10
SR 5
SR 1
AE without absolute value
ESD

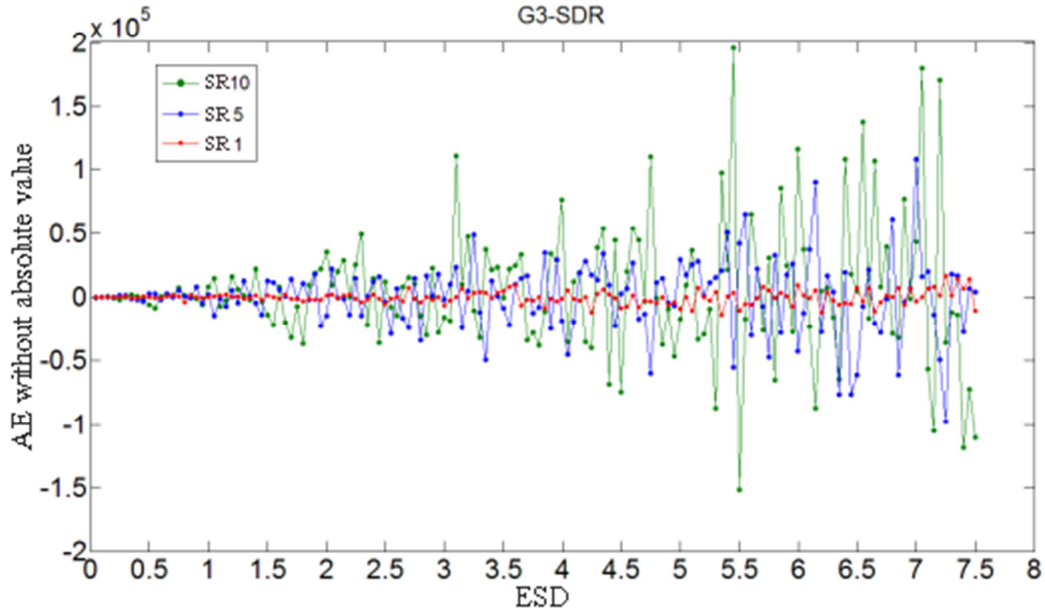
G3-SDR
x 10^5
SR10
SR 5
SR 1
AE without absolute value
ESD

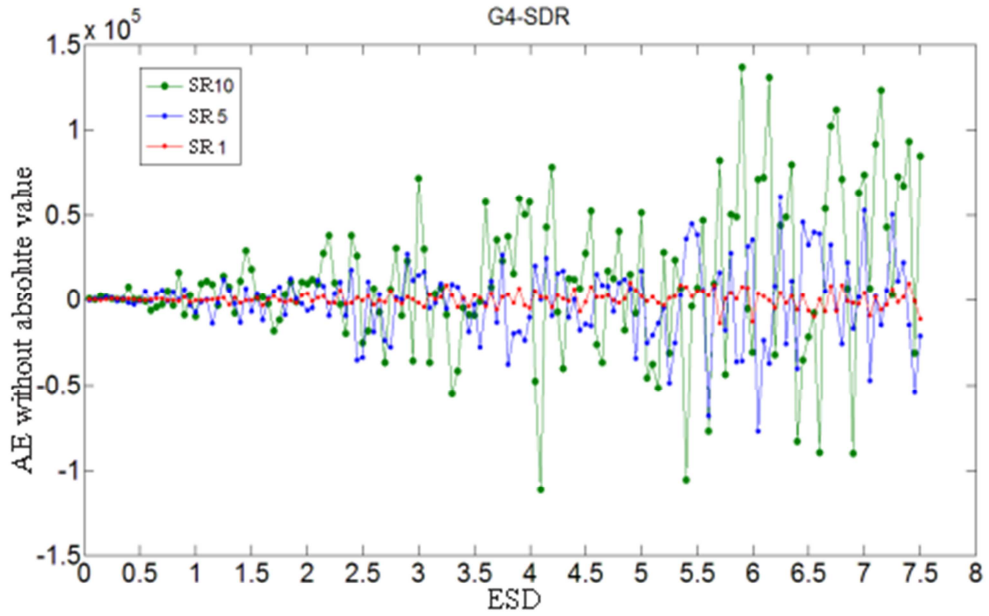

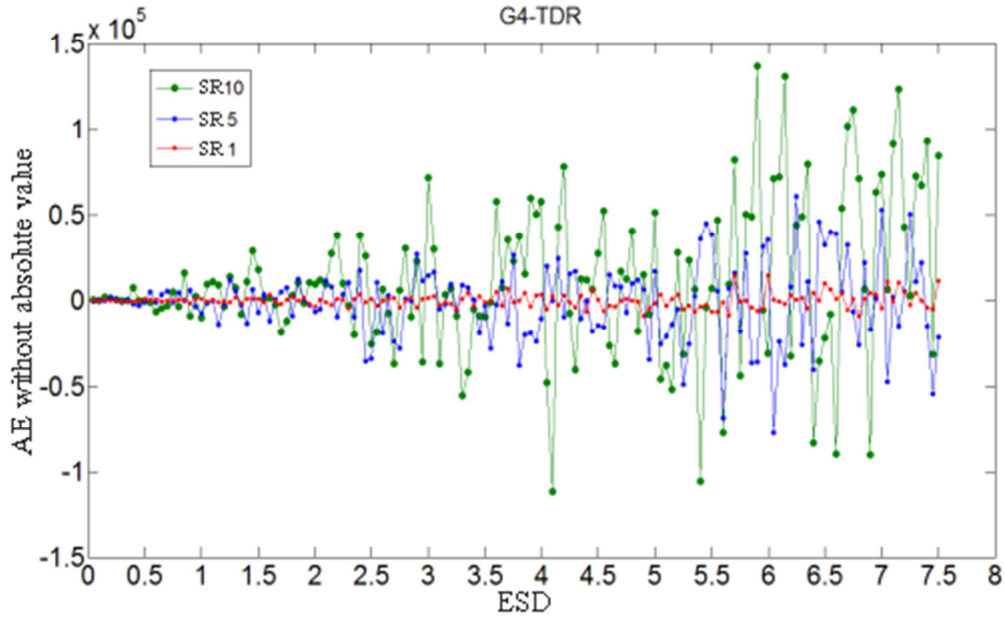

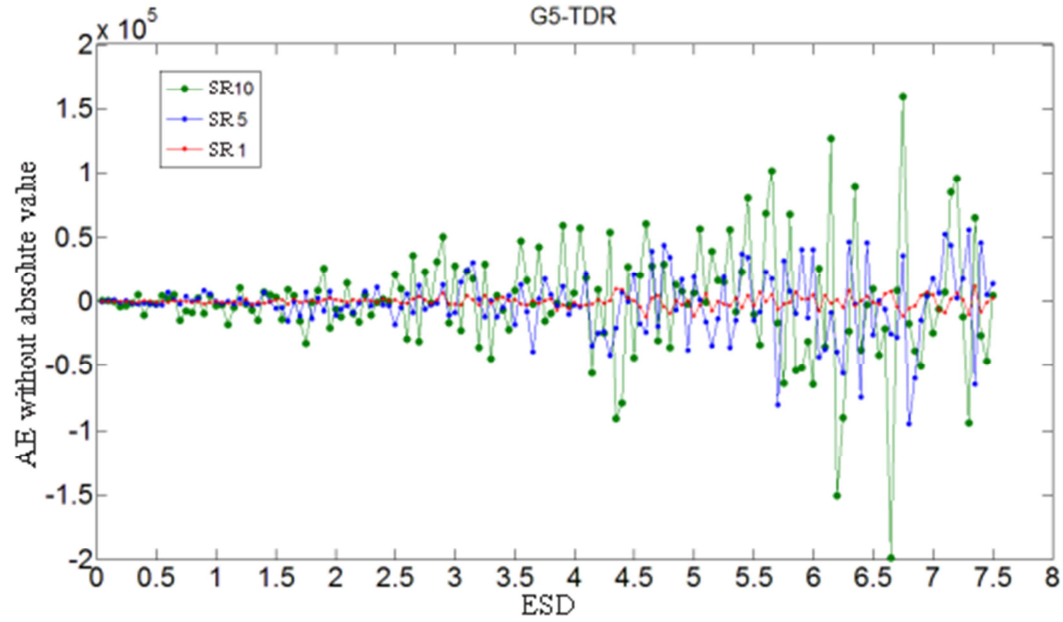
G5-TDR
x 10^5
SR10
SR5
SR1
AE without absolute value
ESD

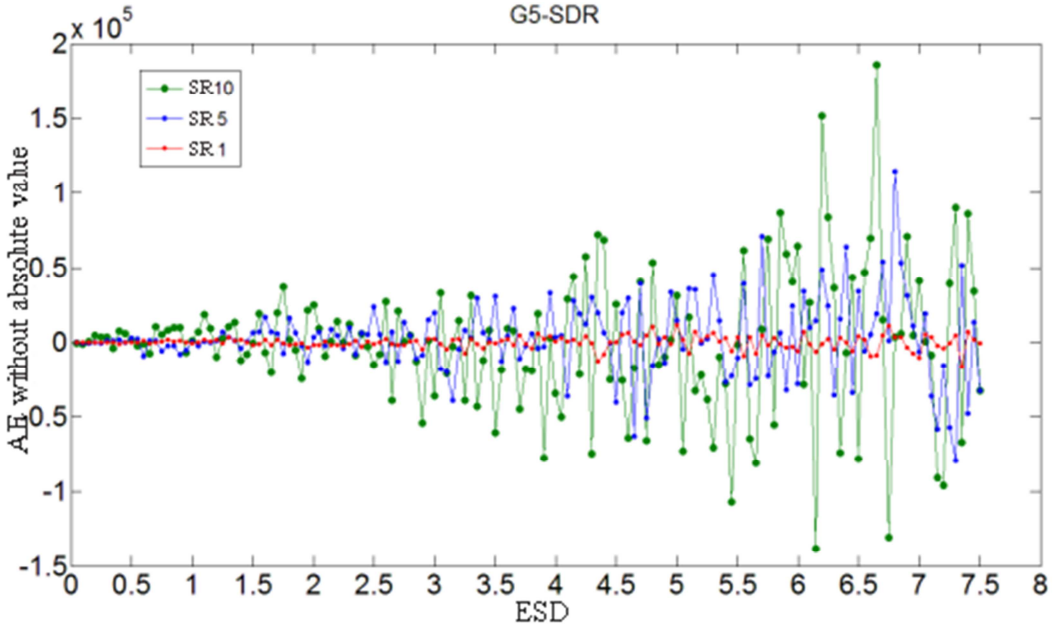
G5-SDR
x 10^5
SR10
SR5
SR1
AE without absolute value
ESD

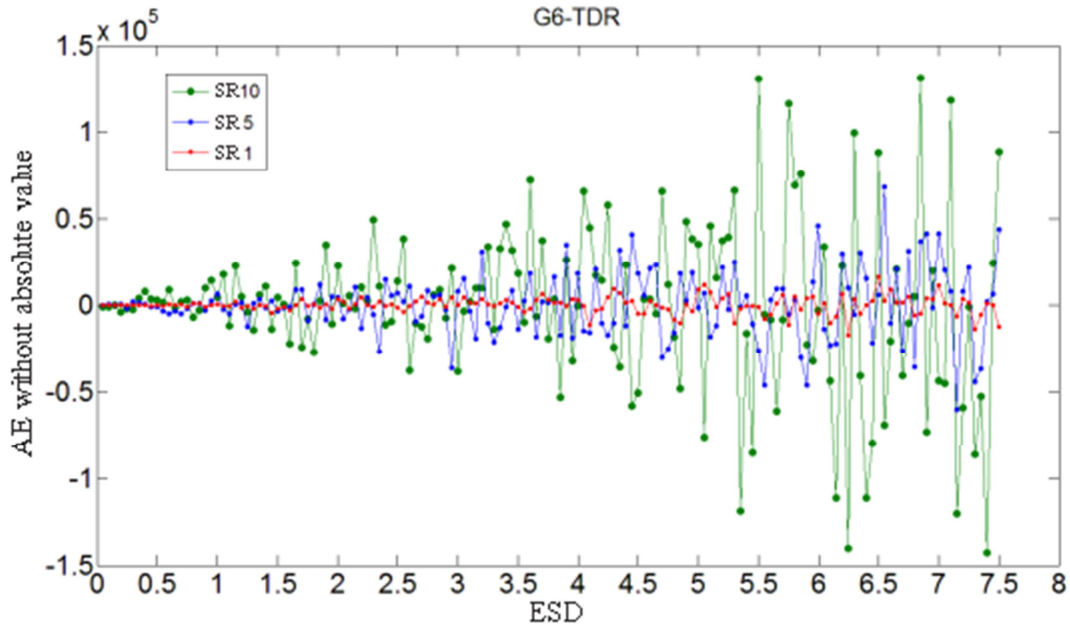
G6-TDR
x 10^5
SR10
SR5
SR1
AE without absolute value
ESD

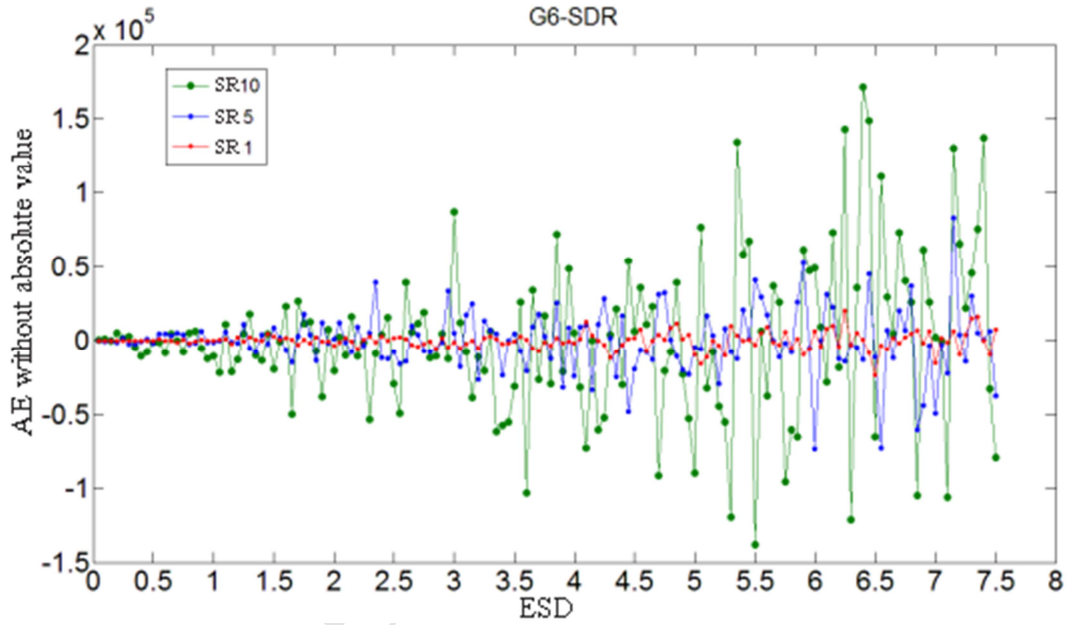
G6-SDR
x 10^5
SR10
SR5
SR1
AE without absolute value
ESD

The main highlights of this paper can be summarized by the following three aspects:

(a) Uncertainty models (truncation errors) of volume calculation are established;

(b) The formula of propagation error is deduced and modelled for volume calculation;

(c) This paper forms a guiding conclusion for volume calculation based on a DEM;